IEEE Access
Multidisciplinary ⋮ Rapid Review ⋮ Open Access Journal

Received 14 July 2022, accepted 29 July 2022, date of publication 8 August 2022, date of current version 26 August 2022.

Digital Object Identifier 10.1109/ACCESS.2022.3197291

TOPICAL REVIEW

Prospect of Using Machine Learning-Based Microwave Nondestructive Testing Technique for Corrosion Under Insulation: A Review

TAN SHIN YEE[1], NAWAF H. M. M. SHRIFAN[2], AHMED JAMAL ABDULLAH AL-GBURI[3], NOR ASHIDI MAT ISA[1], AND MUHAMMAD FIRDAUS AKBAR[1], (Member, IEEE)

[1]School of Electrical and Electronic Engineering, Universiti Sains Malaysia, Engineering Campus, Nibong Tebal, Pulau Pinang 14300, Malaysia
[2]Faculty of Oil and Minerals, University of Aden, Shabwah, Yemen
[3]Department of Electronics and Computer Engineering, Universiti Teknikal Malaysia Melaka (UTeM), Durian Tunggal, Malacca 76100, Malaysia

Corresponding authors: Muhammad Firdaus Akbar (firdaus.akbar@usm.my) and Nawaf H. M. M. Shrifan (nawaf_83@hotmail.com)

This work was supported by the Ministry of Education Malaysia Fundamental Research Grant Scheme (FRGS) under Grant FRGS/1/2019/TK04/USM/02/4.

ABSTRACT Corrosion under insulations is described as localized corrosion that forms because of moisture penetration through the insulation materials or due to contaminants' presence within the insulation material. The traditional non-destructive inspection techniques operating at a low frequency require removing insulation material to enable inspection, due to poor signal penetration. Several high-frequency inspection techniques such as the microwave technique have shown successful inspection in detecting the defect under insulations, without removing the insulations. However, the microwave technique faces several challenges such as poor spatial imaging, large errors in terms of defect size and depth owing to stand-off distance variations, optimal frequency point selection, and the presence of the outlier in microwave measurement data. The microwave technique in conjunction with machine learning approaches has tremendous potential and viability for assessing corrosion under insulation. This paper provides an in-depth review of non-destructive techniques for assessing corrosion under insulation, as well as the possibility of using machine learning approaches in microwave techniques in comparison to other conventional techniques.

INDEX TERMS Corrosion under insulation, machine learning-based technique, microwave non-destructive testing.

I. INTRODUCTION

Corrosion Under Insulation (CUI) is a severe defect in various critical applications, especially in nuclear, marine, aerospace, power generation, and oil and gas industries [1]–[6]. In these industries, the corrosion is grown invisibly in the metal substrate under insulation due to the intrinsic coating imperfections, humidity, and water invasion that makes structural thinning [7]–[9]. This structure's weakness can lead to a catastrophic failure on asset integrity which has several adverse consequences, including production losses, maintenance cost, environmental pollution, and personnel risk in terms of health and safety [10]–[12]. Therefore, an accurate and quick inspection for CUI detection is required to avoid the aforementioned consequences and enhance the system's overall integrity.

Various inspection techniques are commonly used to detect CUI. Among the CUI detection techniques, mass loss measurement [13] is one of the simplest methods to inspect the structure and detect the CUI. The mass loss measurement is based on the weight variation between the defected and defect-free specimens. The weight variation occurs due to the CUI causing significant loss to the weight of the defective structure. However, the mass loss approach can not accurately evaluate the CUI due to no guarantee that the loosed weight is because of the CUI or related to other factors. Moreover, the mass loss inspection is costly and time-consuming due to the cleaning process using alcohol

The associate editor coordinating the review of this manuscript and approving it for publication was Wentao Fan.

and the required drying time, which is not practical in real-world applications [13]. On the other hand, Non-Destructive Testing (NDT)is a promising concept in real-world applications to detect, monitor, and obtain valuable information about CUI severity. An NDT technique can evaluate material integrity for surface or sub-surface defects or metallurgical conditions without interfering in any way with the destruction of the material or its suitability for service [14]. In the industrial sector, there are several types of conventional NDT techniques that are routinely employed, such as Scanning Kelvin Probe (SKP) [15], Giant Magneto Resistive (GMR) [16], eddy current [17] and ultrasonic testing [13]. These conventional techniques have their benefits and drawbacks in terms of safety, expenditures, processing time, and efficiency of the inspected materials. In terms of inspection efficiency, the performance of the aforementioned NDT techniques is degraded due to the field penetration limitation through the dielectric insulations [18], [19].

Recently, microwave NDT has emerged as a promising technique for corrosion detection under dielectric insulations. The electromagnetic waves at a frequency range of 300 MHz – 300 GHz can penetrate the dielectric insulation and interact properly with the metal surface [20]–[23]. The variations in the reflected signals can reveal and evaluate the CUI [22], [24], [25]. Compared to conventional NDT techniques, microwave NDT can perform a non-contact scanning, inexpensive one-side inspection, and it does not require a couplant material or controlled environment to interact with the inspected material. Although these advantages, microwave NDT faces several challenges such as poor spatial imaging due to the stand-off distance variations [26], [27], which reduce the sensitivity of the corrosion detection and locating. Moreover, the nonlinear growth of microwave signal attenuation due to the surface roughness degrades the corrosion level estimation accurately [28], [29]. These microwave NDT challenges still exist because most of the utilized techniques are based on simple signal processing, such as single frequency point selection [30].

Nowadays, several studies have recommended machine learning techniques to improve the inspection quality and reliability of microwave NDT [27], [30]–[33]. Machine learning techniques have an outstanding performance in various real-world applications such as biomedical [34]–[37], image processing [38]–[40], and language processing [41]–[43]. Moreover, machine learning techniques have been successfully used with conventional NDT techniques for detecting and evaluating various types of defects [44]–[46]. The performance of conventional NDT techniques has been improved significantly after utilizing suitable machine learning algorithms for CUI detection [47]–[49]. However, minimal work is conducted using microwave NDT based on machine learning techniques for CUI detection and evaluation [22], [26], [50]. In this paper, the prospect of using machine learning-based microwave NDT technique for CUI is comprehensively reviewed. After presenting the introduction herein, Section 2 discusses the conventional NDT techniques, including their advantages and disadvantages. Section 3 explains the utilized microwave sensors in NDT applications by comparing their processing techniques. Section 4 presents the stages of microwave NDT for CUI detection based on machine learning in terms of pre-processing, features extraction, and classification modules.

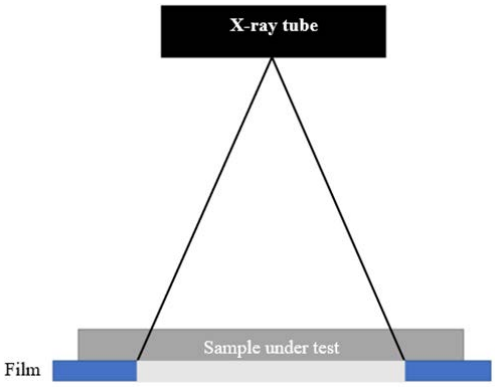

FIGURE 1. X-ray radiography inspection setup.

II. CONVENTIONAL NDT TECHNIQUES

Various conventional NDT techniques are well established in the industry, such as x-ray, thermography, eddy currents, Giant Magneto Resistive (GMR) [16], Scanning Kelvin Probe (SKP) [15], eddy currents [17]. These techniques can be performed on various structures in terms of conductive and non-conductive materials to evaluate different types of defects such as cracks, delamination, and debonding. However, CUI detection and accurate severity evaluation are still challenging for these conventional techniques [5], [22], [51], [52], as discussed in this section.

A. X-RAY INSPECTION

One of the radiography inspection methods for distinguishing the distortion of permeating radiation in materials is the X-ray inspection approach [22]. The X-rays technique uses short wavelength electromagnetic radiation to photograph the structure's profile and determine the thickness of the sample under test [53]. A detector measures the quantity of radiation that goes through the sample being tested. Compared to defect-free locations, voids and discontinuities change the quantity of the received radiations at the detector, which leads to highlighting the thickness variations in the inspected specimen, as shown in Figure 1.

Compton X-ray backscattering approach is utilized in epoxy-coated mild steel to identify and analyze the corrosion undercoating [54]. The thickness variation of the specimen under test is represented by the radiographic image and the typical profile of grey values in the radiographic image. The presence of thickness loss reveals the corrosion damage in the specimen. The degree of corrosion of the test sample is proven by the greyscale image created by scanning the test sample in a stepwise motion. However, the quantitative

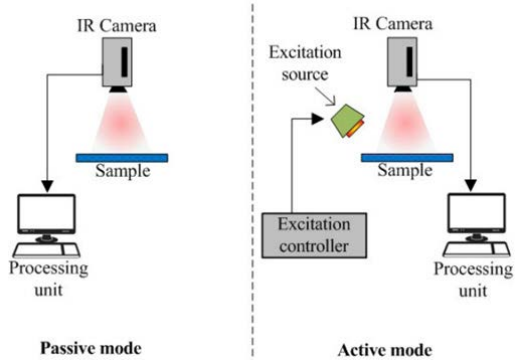

FIGURE 2. Passive and active modes thermography inspection technique [26].

information obtained from the grayscale of the detected corrosion cannot estimate the corrosion level accurately. Moreover, performing X-ray inspection requires protection due to the long exposure to X-ray radiation leads to health and safety implications [55].

Employing machine learning in X-ray inspection approach is feasible to accurately detect and cluster the corrosion and corrosion-free regions. Linear Discriminant Algorithm (LDA) is used in X-ray photoelectron spectroscopy technique for classifying the defect area of copper cylinder coated with epoxy resin [56]. LDA is a common preprocessing approach for dimensionality reduction to find a linear projection of high-dimensional observations into a lower-dimensional space [57]. In addition, LDA can define optimal linear decision boundaries in the resulting latent space for pattern classification applications [58]. The study presents 81.6 % accuracy in discriminating between the corrosion and corrosion-free regions in the copper undercoating.

B. THERMOGRAPHY INSPECTION

The thermography inspection approach can eliminate the health and safety issues due to radioactive sources. This approach is another NDT technique for observing the temperature distribution of the Sample Under Test (SUT) [59]. The temperature distribution is captured using an infrared camera that sensitive to small thermal variations. Thermography inspection techniques are classified into passive and active thermography, as shown in Figure 2 [26]. The passive thermography analysis is performed under the two mediums in thermal disequilibrium, while the active thermography is performed by modifying the temperature of the medium using artificial heat sources such as a lamp, laser, and ultrasonic. The shape of the defects is detected as different temperature distributions compared to the non-defect area.

An active thermography inspection approach with a heat chamber is used in the metal shingles to detect and analyze the corrosion without removing the coating layer [60]. This technique is applied to inspect metal with the coated paint layer. The thermal contrast is recorded and analyzed by the Maximum Normalized Temperature Difference (MNTD) analysis. The MNTD analysis aims to obtain the temperature difference between the corroded and non-corroded regions. The finding shows that the thermal contrast changes with the presence of corrosion. This technique is a non-contact inspection technique. It is possible to track high temperatures and hazardous objects safely [61]. However, the thermal contrast between the corroded and non-corroded areas is influenced by the type of coatings.

In terms of active thermography, Pulsed Thermography (PT) is less influenced by the type of coatings. The PT technique is a rapid NDT technique for heating the surface of SUT using a high-intensity pulse of light [62]. This technique is applied to inspect epoxy coating with ceramic flakes [63]. A sequence of thermograms is obtained and used to inspect the corrosion undercoatings. The study presents that all the CUIs with different coatings are detected. In addition, the changes in thermal contrast between the defects in either the coating layer or metal layer present a significant success. However, there are no significant changes in the thermal contrast between flat and conical bottom holes. Hence, the PT technique cannot significantly determine the form of the CUI and, worse yet, the CUI depth. Moreover, thermography NDT provides less quantitative information about sub-surface defects in the case of thick insulation layers [30].

Grosso *et al.* [63] deploy the Finite Element Model (FEM) for the post-processing of the defect identification in this study to determine the shape of the CUI [63]. FEM is a computation approach that has been used to find approximate solutions to differential equations [64], [65]. The FEM subdivides a large system into smaller, simpler parts called finite elements. The FEM model aids in determining the diameter of the defects in this investigation since the diameter of the defects impacts the temperature value presented as well as thermal contrast. The thermal contrast between flat and conical bottom hole defects is effectively shown using the FEM model. This research also shows a good correlation between the experimental and simulated data. On the other hand, the FEM model is unable to classify the defects as it is not a clustering algorithm.

Machine learning algorithms have been employed in the infrared thermography approach to classify defects. A Perceptron Neural Network (PNN) model is hybridized with the pulsed infrared thermography approach for classifying the corrosion and corrosion-free regions in the aluminum with fiberglass coating automatically [55]. PNN is a feed-forward neural network used to learn and classify the input vectors into the class with the most similar characteristics [66]–[68]. The PNN model succeeds in yielding 94 % corrosion classification. However, owing to heat dispersion from the surrounding defects, there are still inaccuracies in the classifications of non-defect zones. The edges of the corrosion are also incorrectly characterized. In addition, to train well-performing models, the PNN model necessitates a large number of training samples.

In order to reduce the detection error rate using significant contrast, CNN is employed with thermography inspection

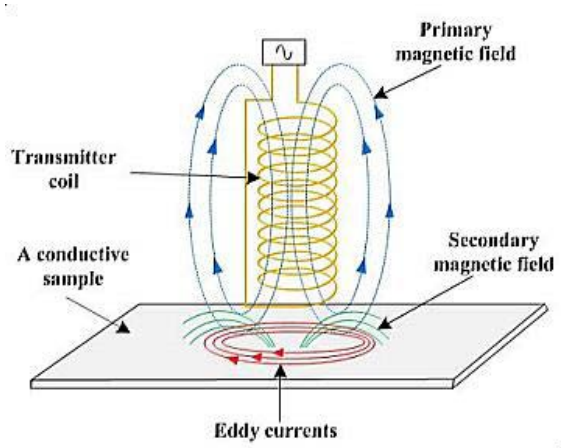

FIGURE 3. The principle of eddy current [26].

to classify the defect and non-defect area in Carbon Fiber Reinforced Polymers (CFRP) sample [69]. The thermography inspection result can be distinguished depending on the temperature variation between the defect and defect-free components. The results illustrate that the CNN model improves defect identification by generating a clearer contrast between the defect and defect-free areas. Additionally, the CNN model is more resilient to thermal signal distortions, which are ambient noise and non-uniform heating. However, the CNN model requires a massive training sample to train a relatively accurate model.

C. EDDY CURRENT TESTING

Eddy Current Testing (ECT) technique can provide quantitative information such as the depth of CUI. The ECT approach is commonly used for inspecting the conductive materials in heavy industries to detect surface and subsurface defects [70], [71]. A primary transmitter coil is used in the ECT probe to establish magnetism surrounding the inspected metallic location, as shown in Figure 3 [26]. As a result, eddy currents are induced on the metallic specimen. The eddy currents generate a secondary magnetism that is polarized in the opposite direction as the source field [72]. In the case of defect presence, eddy currents become weak and influence the secondary magnetic field [73]. The difference in the magnetism is measured using a coil or a magnetic sensor to differentiate between the defect and defect-free locations.

In terms of CUI, the method concept in [74] has employed ECT to predict the level of corrosion in insulated steel plates. The amplitude of obtained signals is normalized and used to represent the level of corrosion. The CUI is clearly observed due to the linear correlation between the level of CUI and normalized signals' amplitude. However, a pre-knowledge is required to select the efficient parameters that can effectively represent CUI [75]. Moreover, the ECT is sensitive to lift-off variations between the probe and the inspected surface, which degrades the depth penetration [76], [77].

Pulsed Eddy Current (PEC) technique is proposed to enhance the penetration of Eddy current [72]. The pulsed magnetic field used can penetrate between the probe and Sample Under Test (SUT) via any non-magnetic substances. It improves the penetration depth of CUI inspection for different depths by applying a single pulse [72]. PEC is used to examine the presence of CUI in the gas pipeline [78], [79]. In this case, the signal amplitude represents the depth of the corrosion. The study shows that conventional EC testing can predict the depth of CUI, but PEC can enhance the penetration depth of the magnetic field. However, there is a limitation on the lift-off distance for the measurement, which affects the accuracy of the measurement. The PEC technique needs to be carried out the measurement in the Lift-Off Intersection (LOI) area to eliminate the lift-off distance effect.

Leveraging the PEC technique, a supervised machine learning algorithm has evolved to improve the measurement accuracy of a predicted thickness of the sample [80]. This work employs Gaussian Process Regression (GPR) model to predict the wall loss in coated carbon steel sample, which illustrates the corrosion under insulation. GPR model is a non-parametric, Bayesian approach to modeling the uncertainty of the prediction [81], [82]. GPR model calculates the probability distribution over all functions that fit the data [83], [84]. The experimental result with the GPR model achieves lower nominal errors and error variances. This framework also improves the scanning speed and reduces the inspection time of the sample. However, larger datasets increase the evaluation time of the sample. In addition, the accuracy of the prediction decreases.

D. GIANT MAGNETO RESISTIVE

Giant Magneto Resistive (GMR) is usually used to inspect the surface and subsurface defects in conductive and magnetic materials [85]. GMR employs a ferromagnetic layer in which the electron orientation is easily manipulated by applying an external magnetic field [86]. In NDT, the GMR sensor is usually implemented as a magnetic receiver in the ECT technique to increase the sensitivity of small defect detections [87], [88]. The magnetic moment of GMR sensor ferromagnetic layers is aligned with the secondary magnetic field generated by eddy currents, which overcomes antiferromagnetic coupling [89]. As a result, the resistance to current is low. In the presence of CUI, the secondary magnetic field established by eddy currents becomes weak. The magnetic moment of both GMR ferromagnetic layers is in the opposite direction owing to antiferromagnetic coupling, resulting in high resistance. GMR sensor can directly measure the magnetic field changes [87]. Figure 4 depicts the mechanism of the GMR sensor with an external magnetic field.

Eddy current array technology is presented to improve the penetration of Eddy current. It uses a very low-frequency eddy current with GMR sensing elements to illustrate CUI of thick aluminum weather jacketing pipes with quicker and high-resolution images [73]. By changing the eddy current to a very low operating frequency, the sensor arrays can cover more expansive areas while maintaining the traditional eddy current testing technique's advantages. The study shows that

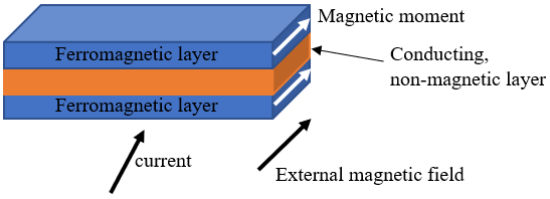

FIGURE 4. Mechanism of GMR sensor with an external magnetic field.

the magnetic fields from a larger spatial wavelength sensor penetrate further into the SUT at low frequency. By using the magneto resistive sense element mounted on a sensor, the sensitivity and speed of measurement of the scanner increased. In this case, a C-scan image is used to inspect the corrosion under coatings of the inspected pipelines. The eddy current sensor array with magneto resistive sensing elements presents a big success in inspecting the CUI. The sensor succeeds in inspecting the diameter of the area of corrosion under coatings. However, manually shifting the sensor is a must for wide scanning areas. In addition, the size and weight of this sensor is the limitation for hand-carry.

The use of supervised machine learning in the eddy currents with the GMR method has improved the accuracy of corrosion and corrosion-free regions classification [88], [90]. The study utilizes Support Vector Machine (SVM), Naïve Bayes, logistic regression and random forests to classify the CUI and CUI-free areas to examine the corrosion in the coated cast-iron pipeline [90]. The research presents an excellent classification result of corrosion and non-corrosion zones, with the SVM classifier achieving the best classification. 90 % classification accuracy is obtained using the SVM algorithm. However, supervised machine learning approaches need a huge amount of training sets in order to construct a more accurate model.

E. SCANNING KELVIN PROBE

In terms of Scanning Kelvin Probe (SKP), it is commonly employed to determine the coating failure of poorly conductive materials instead of conductive materials by measuring the work function or Volta Contact Potential Difference (V_{CPD}) of the material [91], [92]. SKP utilizes a Kelvin probe near the surface of the specimen to form a capacitor, as shown in Figure 5 [9].

The contact potential is generated between the surface of the Kelvin probe and the sample. The V_{CPD} between the conductive vibrating tip and sample is brought into equilibrium [93]. In the case of CUI presence, the differences in V_{CPD} occur and the probe's vibration induces Alternating Current (AC). The induced AC is measured at the resistor, R_{IN}, to obtain the value of V_{CPD} [24]. The corrosion potential of the sample interface impacts and varies linearly to the V_{CPD} [95].

The atmospheric corrosion of epoxy resin-coated galvanized steel is studied using the method concept in [91].

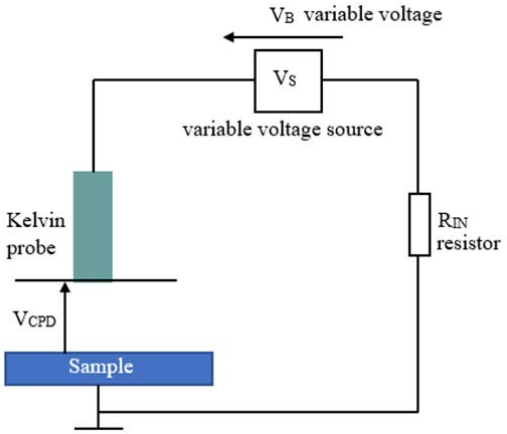

FIGURE 5. Scanning kelvin probe (SKP) technique.

The V_{CPD} surface distribution is obtained and plotted to measure the corrosion potential. The regularity of the V_{CPD} distribution is affected when CUI is present. SKP presents a useful method for accessing the spatial separation of the electrochemical reactions at the interface of the defect and the surrounding metal or paints in this study. However, the defect obtains a more positive potential profile value compared to the topography of the same area. The accuracy of the inspection of CUI depth is low.

SKP method is proposed in a different way to enhance the potential profile value of SKP [96]. It is applied in epoxy-coated carbon steel to illustrate the uniformity of the CUI. The Variation Coefficient (VC) of the V_{CPD} is used to eliminate the issue of positive potential value. The VC is the deviation of the average V_{CPD} from the mean values of each sample. The VC at various exposure times is used to illustrate the variations over the sample graph. It can be concluded that the lower the VC value, the more uniform the CUI. Hence, SKP succeeds in detecting CUI. However, the capacitance between the probe and conductive substrate may differ as the coated steel is exposed to the corrosive aqueous medium. The V_{CPD} is therefore affected.

The SKP approach employs unsupervised machine learning to classify the corrosion and corrosion-free areas. The k-means clustering algorithm is employed to categorize the corrosion under the insulation of coated low-carbon steel [97]. The k-means algorithm clusters the corrosion under insulation based on the surface potential of the sample obtained using the SKP technique. The study presents a k-means clustering algorithm managed to classify the corrosion and non-corrosion zones. However, the clustering images appear noisy. In addition, some of the regions are improperly clustered. This is because of the local signal fluctuations in the detected surface potential.

F. ULTRASONIC INSPECTION

Ultrasonic Testing (UT) is utilized to enhance the inspection of CUI depth. UT is often employed in sound conducting

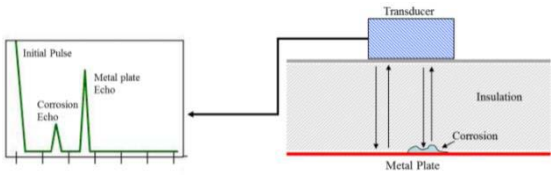

FIGURE 6. Ultrasonic inspection [94].

materials to examine internal corrosion [98]. UT employs an ultrasonic transducer to induce ultrasound waves toward the Sample Under Test (SUT) [94], [99], as shown in Figure 6. The Time Of Flight (TOF) of ultrasonic reflected waves is used to calculate the metal losses of the internal and external surfaces [100]. Hence, it is usually used for thickness measurement and corrosion monitoring.

Ultrasonic testing with the CNN model is introduced in stainless steel specimens to image the defects at the bending part of the pipe [101]. CNN is a deep learning algorithm that can compile the retrieved reduced characteristics into a high-level depiction [102]. CNN is also capable of analyzing an input image, determining the significance of different attributes and distinguishing between them [103]. An automated system based on damage detection of pipe bend is achieved. The results prove that a normalized rate of detection of 89 % is obtained. The misdiagnosis defects are due to no discernible difference in color or juxtaposition between the subject and the surrounding. However, conventional ultrasonic testing suffers from weak wave reflection from a thin metal substrate coated with a thick coating.

Compared to conventional ultrasonic inspection, Phased Array Ultrasonic Testing (PAUT) uses multiple elements to induce and receive ultrasound pulses in a single transducer for surface and near-surface inspection [104]. This transducer can scan, steer and focus the beam at different angles over the inspected material [105]. The received signals obtained by the multiple elements are summed together and recorded for further analysis. The PAUT commonly employs C-scan to illustrate the inspected sample in 2D images. PAUT inspection is faster and able to cover a larger area compared to conventional ultrasonic inspection [106].

In terms of corrosion detection, Phased Array Ultrasonic Testing (PAUT) is used to detect the corrosion-under-paint in a carbon steel substrate [104]. C-scan is employed to image the corrosion undercoating of the sample. The corrosion under 1 mm paint thickness is successfully identified and located. However, the boundaries of the detected corrosion are not clear enough to accurately measure the defect size. This is due to the non-smooth corroded surface of the specimen, making the defect size assessment challenge. Moreover, the conventional PAUT requires gel or water as couplant to inspect a specimen surface which is insatiable for a specimen that cannot be immersed.

Machine learning is also being emerged in the PAUT inspection to detect the presence of defects precisely. In order to identify the corrosion in the coated aluminum block, a Convolutional Neural Network (CNN) is trained and employed [107]. CNN model learns the characteristics of the representations from data and delivers a data output based on previous knowledge [108], [109]. According to the findings, the CNN model can identify all of the corrosion zones with additional training using a small amount of experimental data. However, the CNN model requires a massive training sample to train a relatively accurate model.

Table 1 summarizes an evaluation of numerous conventional NDT techniques. The conventional NDT techniques detect the CUI with low accuracy. The emergence of machine learning approaches in conventional NDT techniques helps in identifying and distinguishing the CUI and CUI-free areas with higher precision. In addition, the inspection time is reduced.

In inspecting CUI, the main limitation of the aforementioned techniques is the field penetration through the coating layer, as shown in Table 1. The coating layer changes the standoff distance between the sensor and the metal substrate, making deep field evaluation a challenge, especially in composite coatings [110]. Although machine learning approaches have improved the inspection quality of the aforementioned techniques, an alternative NDT technique is required to handle the field penetration limitation of the conventional NDT techniques for further improving the CUI evaluation.

III. MICROWAVE NDT

Compared to the conventional NDT, microwave NDT is a powerful technique for inspecting the under-coating defect such as CUI. Electromagnetic waves at electromagnetic frequencies (300 MHz- 300 GHz) can deeply penetrate the composite insulation and are sensitive to the thickness changes in the surface of the metal substrate [26], [111], [112]. The microwave NDT technique provides several advantages, such as non-contact inspection, and does not need a couplant for the signal transmission into the sample under test [113]–[116]. The microwave NDT technique has prompted the search approach for inspecting the defects within and under the composite materials. Microwave impulses, unlike ultrasonic waves, can propagate through the composite structures' insulation and interface with underlying structural materials [18]. In microwave NDT, the magnitude and phase of the transmitted and/or reflected waves are commonly used to evaluate the Sample Under Test (SUT) [117].

Among microwave waveguides, an Open-Ended Rectangular Waveguide (OERW) is frequently employed to inspect metal surfaces coated with dielectric and composite materials. Hence, OERW is usually used to examine the defects such as delamination, crack, and CUI. The OERW induces the microwave signal towards the SUT. The shift in resonant frequency, magnitude and phase of the reflection coefficient of the microwave signal is used to image the defects. A sweeping frequency is in the microwave NDT techniques presented in [24]. The OERW probe is operated in K-band to evaluate the coated atmospheric corrosion on mild steel.

TABLE 1. Comparison summary of various conventional NDT techniques.

Ref. No.	Technique	Concept of use	Advantages	Disadvantages
[54]	Compton X-ray backscattering	CUI evaluation on coated mild steel	- Inspect the thickness loss of the sample under test. - Able to present the degree of corrosion.	- Unable to provide quantitative information for depth of CUI. - Hazard to health.
[56]	X-ray-LDA	CUI clustering in epoxy resin caoted copper	- Dimensionality reduction. - Able to discriminate corrosion and corrosion-free regions.	- Cannot work well with high dimension.
[60]	Active mode IRT	Corrosion detection in coated paint layer metal shringles	- Inspect the corrosion with thermal contrast. - Non-contact technique. - Able to inspect high temperature and hazardous samples safely.	- The thermal contrast is affected by type of coatings.
[63]	IRT-PT	CUI and defect detection in the epoxy coating with ceramic flakes	- Able to detect CUI in different coating materials. - Able to detect the location and type of defects.	- Unable to detect the shape and depth of CUI.
[63]	IRT-PT-FEM	CUI shape determination in the epoxy coating with ceramic flakes	- Able to determine the diameter of CUI. - Able to determine the shape of CUI. - Good correlation between experimental and simulated data.	- Unable to cluster the CUI and CUI-free regions.
[55]	IRT-PT-PNN	CUI clustering in aluminum with fiberglass coating	- Able to classify the CUI and CUI-free regions.	- Inaccuracies in classification of non-CUI zones. - Huge amount of training samples are required to train the model.
[69]	IRT-CNN	Defect classification in CFRP sample	- Able to generate a clearer contrast between defect and defect-free areas. - More resilient to thermal signal distortions.	- Massive training samples are required to train accurate model.
[74]	ECT	Prediction of corrosion in insulated steel plates	- Sensitive to surface detects. - Predict CUI accurately by normalized signals' amplitude.	- Pre-knowledge is required to represent CUI effectively. - Sensitive to lift-off distance between the probe and inspected sample's surface.
[72]	ECT-PEC	CUI mapping of gas pipeline	- Fast CUI inspection. - Achieve corrosion mapping. - Achieve the determined penetration depth of the magnetic field.	- Measure LOI area to eliminate lift-off distance effect.
[80]	ECT-PEC-GPR	Wall loss prediction in coated carbon steel	- Able to predict the wall loss with lower nominal errors and error variances. - Improve the scanning speed. - Reduce the inspection time.	- Large datasets increase the evaluation time. - Large datasets decrease the prediction accuracy.
[73]	ECT-array with GMR sensing elements	Imaging of CUI for thick aluminum weather jacketing pipes	- Able to inspect more expansive areas. - The high sensitivity and fast measurements. - Penetrate further into SUT at low frequency. - Flexible.	- Manually shift for wide scanning areas. - Bigger in size and heavier.
[90]	ECT-GMR-SVM	CUI classification in coated cast-iron pipeline	- Able to classify the CUI and CUI-free zones accurately.	- Huge amount of training samples are required to train the model.
[91]	SKP	Corrosion detection in epoxy resin-coated galvanized steel	- Determine the spatial separation of electrochemical reaction at the corrosion. - Corrosion is detected by using topography and the potential profile of the sample surface.	- The defect obtains a more positive potential profile value than topography of the same area. - The accuracy of CUI depth inspected is low.
[96]	SKP	Corrosion detection in epoxy coated carbon steel	- Able to detect the uniformity of the CUI. - Eliminate the positive potential value issue.	- The capacitance may differ and affect the Volta contact potential.

TABLE 1. *(Continued.)* **Comparison summary of various conventional NDT techniques.**

[97]	SKP-k-means	CUI classification in coated low-carbon steel	- Able to classify CUI and non-CUI areas.	- Clustering images appear noisy. - Some regions are improperly clustered.
[100]	UT	In-Line Inspection (ILI) for CUI underground	- Calculation of metal losses using TOF of the reflected ultrasonic signal.	- A coupling medium is required. - Not capable of giving detailed data of thickness loss.
[101]	UT-CNN	Defects detection of stainless steel bending pipe	- Automated damage detection of pipe bend.	- Incorrect defect detection due to no discernable difference in color between the subject and surrounding.
[104]	UT-PAUT	Corrosion detection in carbon steel with paint coating	- Multiple elements are used to scan, steer and focus the beam with a single transducer. - Produce clearer images over the microwave imaging system.	- Complex. - Expensive than a microwave imaging system. - Boundaries of detected corrosion are not clear. - Require gel or water as couplant. - Unable to use with specimen cannot be immersed.
[107]	UT-PAUT-CNN	Corrosion identification in coated aluminum block	- Able to identify all the CUI areas.	- Huge amount of training samples are required to train the model.

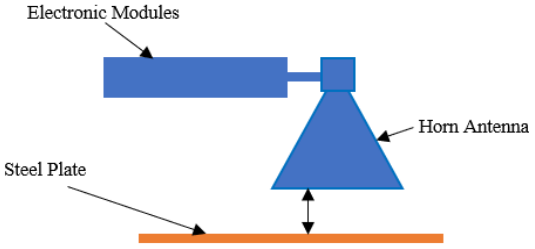

FIGURE 7. Experimental setup of horn antenna microwave NDT technique [59].

The 2D vision is constructed using the average magnitude and phase of the reflection coefficient. In this case, average magnitude offers a more accurate depiction of CUI detection as the phase has been influenced by the surface's roughness and is more sensitive to lift-off distance. Moreover, OERW provides high-resolution, non-contact and intuitive images. It has the advantage of short processing time compared to the conventional NDT techniques. However, relatively high-cost microwave equipment is the drawback. Hence, this proposed technique has shown the potential for inspecting, imaging and monitoring CUI.

A horn antenna is another microwave sensor that provides high gain and wide bandwidth for varying frequencies [59]. It is often used to inspect metal sheets coated with dielectric and insulation for delamination, crack, and CUI. The horn antenna transmits and receives the microwave signals to or from the SUT. Similar to the OERW, the alteration in resonant frequency as well as the magnitude and phase of the reflection coefficient of the microwave signals to image the defects.

A pyramidal horn antenna with a rectangular waveguide is used as the microwave sensor to inspect the CUI in steel plate with paint coatings [59]. Pyramidal horn antennas are typically fed by rectangular waveguides and flared in electric fields and magnetic fields to ensure that both fields are similar. Frequency Modulated Continuous Wave (FMCW) radar transmits an electromagnetic signal but does not continuously sweep the frequency. Figure 7 illustrates the experimental setup. The 2D image is obtained at the waveguide aperture by using the phase difference between the sent and received signals. In the presence of CUI, the phase of the signal responses is changed. The significant signal changes to signify the corrosion area are due to the corrosion's permittivity change. The phase shift is capable of illustrating the depth of CUI. The ability to move the sensor with respect to the sample surface is another advantage over conventional NDT techniques. However, some phase shifts and variations in amplitude among the healthy data are due to the aluminum flakes in the paint and the poor coating application. In addition, it will be better if the sensor can focus the beam at a more concentrated angle, allowing much smaller corrosion to be detected.

There has been substantial research and development using Radio Frequency Identification (RFID) for examining the CUI. RFID is used to inspect the steel corrosion sensing and characterization under insulation. RFID utilizes radio frequency to transfer power and data between a reader and a tag [94]. The reflected signals from the SUT are measured to image the defects. RFID sensors are classified into passive and active sensors. The reader's signal supplies power to the passive RFID sensors. In contrast, the signals transmitted by active RFID sensors are powered by themselves and capable of delivering a more readability range than passive RFID sensors [118].

A chipless RFID sensor is applied to monitor the pipeline coating by detecting the concentration of salty water ingress in the pipeline coating [119]. The data of S_{21} (transmission coefficient) is measured using Vector Network Analyser

(VNA). The amplitudes of the measured S_{21} are plotted to illustrate the variations over 2D imaging using various salty water ingress concentrations. Thus, the finding presents that the detection of the concentration of water salinity level can act as an early prediction for CUI. The CUI can be precisely estimated compared to the IRT technique by the water salinity level with the simple detection of water presence. However, the challenges such as tag localization, read range extension and tag detection are required to be overcomed so that it can be widely deployed.

Furthermore, Spiral Ring Resonator (SRR) is one of the MNDT techniques commonly used to inspect the coating defects such as liquid ingress or air breach wirelessly. SRR generates a high-isolation band-stop filter frequency. In the case of defect presence, the resonant frequency is relocated in accordance with the degree of the damage. A 55-element array of exactly similar and symmetrical Rectangular Spiral Ring Resonators (RSRR) coupled with a transmission line is employed to detect the water ingress in the insulation layer for the early prediction of CUI [120]. The data of measured S_{21} is measured using VNA. The 2D image is obtained using the amplitudes of the measured S_{21}. The study demonstrates that the shifting of the resonant frequency represents the amount of water ingress. The amount of water can be identified by using this technique compared to the IRT technique. The RSRR sensors are low profile, tunability and small size compared to other microwave sensors. However, the separation between the array members and the number of elements in the array should be investigated to optimize the sensor's performance.

In addition, Guided Microwave Testing (GMT) is frequently used to analyze a significant proportion of the pipeline. GMT employs the cladding and insulated pipeline as a coaxial waveguide to promote the propagation of electromagnetic waves. In the defect presence, the impedance discontinuities occur in the waveguide, causing the reflection of the incident microwave signal. Hence, the defects are detected and located. GMT is applied to detect the wet insulation in insulated galvanized steel ducting pipes [121]. The amplitude of the reflection coefficient of the signal is used to represent the level of water ingress. 2D image is obtained utilizing the amplitudes coefficient. The finding presents that the sensor shows high sensitivity towards the volume of water. Compared to other techniques, GMT is more suitable to apply in long-range inspection for the pipeline. However, the water not only grows in one direction, and it is hard to predict the water path. Hence, more attempts should be made to model the realistic scenario of the growth of water in the insulation layer. Besides, replacing the foam block with composite materials are necessary to obtain an accurate result.

Microwave NDT techniques are superior compared to conventional NDT techniques in terms of field penetration through the insulation, short processing time and high-resolution images. Non-contact is one of microwave NDT's advantages as the UT technique requires a coupling medium. Compared to conventional NDT techniques, the CUI depth can be indicated by phase shift and moving the sensor over the sample surface using microwave NDT. In addition, conventional NDT techniques can only detect the water presence, whereas microwave NDT techniques can detect the volume of water presence. This technique possesses the capability to increase the precision of early CUI detection.

Table 2 summarizes an evaluation of numerous conventional microwave NDT approaches. Among all the microwave sensors discussed, OERW operated in K-band shows an outstanding result in detecting CUI by using multiple operating frequencies. Short processing time is an advantage for OERW as it can produce high-resolution images simultaneously. However, the entire corrosion area is challenging to get since the thickness of the corroded area is very thin. It requires high-cost microwave equipment to operate. Besides that, as a result of stand-off deviations and the appropriate frequency range to be chosen, the output of OERW is degraded [122]. Therefore, to attain the best possible image resolution and assessment reliability for CUI, the outliers and noise must be removed by signal processing approaches.

IV. MICROWAVE NDT-BASED MACHINE LEARNING

Conventional NDT techniques still face some limitations, such as poor spatial imaging, field penetration limitation, and blurred defects shape, which reduce the quality of inspection of CUI. The recent research field is particularly reliable on the developments of NDT automation. This minimizes the dependence on the operators' understanding and expertise. Thus, signal processing with machine learning classifiers is employed in NDT techniques to enhance the reliability of the inspection of CUI. Moreover, it can improve the prediction rate of the CUI level.

NDT technique based on the Machine Learning (ML) approaches commonly passes via three stages: pre-processing, feature extraction, and classification [123]. In the pre-processing stage, a set of steps are executed prior to data analysis which aims to refine and eliminate unnecessary data to minimize the analysis errors. On the other hand, the feature extraction stage aims to obtain several informative features from a large set of data for better data interpretation. In terms of the classification stage, the extracted features are classified using a machine learning classifier to group similar data into several classes, such as defect and defect-free. Machine learning clearly shows remarkable improvement in simulation and data processing. ML-based models have demonstrated a good forecast precision and strong ability for fitting analysis. ML is used for configuration simplification, structure supposition, fault performance assessment, experimental development over recent years, and materials science [127]. The ML-based models used in CUI are to detect, image, and evaluate the severity of CUI or compute the CUI defect depth growth rates and estimate the failure probability. In the following subsections, various algorithms that are commonly used in the three stages are discussed.

TABLE 2. Relative overview of the conventional microwave NDT approaches.

Ref. No.	Technique	Concept of use	Advantages	Disadvantages
[24]	OERW operated in K-band	CUI evaluation on coated mild steel	- Multiple operating frequencies can be applied. - Non-contact. - High-resolution image. - Short processing time.	- High cost of microwave equipment. - Hard to obtain the whole corrosion area if the thickness of the corroded area is very thin.
[59]	Horn antenna with rectangular waveguide	Microwave-based monitoring system for CUI	- High gain. - Wide bandwidth. - Able to illustrate the depth of CUI.	- Better if smaller corrosion can be detected.
[119]	Chipless RFID	Detect salty water ingress in pipeline coating	- Passive and wireless sensor. - Predictive approach for CUI by the water salinity level.	- Two linearly polarised antennas need to be placed perpendicularly to each other to avoid crosstalk.
[120]	RSRR coupled with transmission line	Detect water ingress in the insulation layer	- Early detection for CUI. - Real-time CUI prediction monitoring.	- Long in size as 55-elements array of RSRR is used.
[121]	Guided Microwave Testing (GMT)	Detect wet insulation in pipes	- Early detection for CUI. - Suitable to be applied in long-range pipeline inspection. - The sensor shows high sensitivity towards the volume of water.	- The experiment was carried out by using a foam block. - Prediction of water in one direction.

A. PRE-PROCESSING

In this section, only well-known pre-processing techniques are discussed as an example for the signal processing stage, such as Discrete Wavelet Transform (DWT), Hilbert Transform (HT), and Variational Mode Decomposition (VMD). DWT is a discretized Wavelet Transform (WT) for identifying and removing the electrical noise from the signals [128]. WT splits a stream of data into numerous levels reflecting distinct bandwidths [30], [129]. The position of the WT at each scale determines the electrical noise. A threshold is defined with the noise information. The noise is removed effectively by eliminating the threshold value below the threshold. In detecting the miniatured delamination in the coated Perfect Electric Conductor (PEC), the DWT technique is used to filter out background noise from the signal obtained using a dual-ridges OERW [124]. The DWT is applied in conjunction with the intensity analysis of the signal to predict the delamination's depth. By applying the DWT signal denoise, the estimation of the defect depth is significantly accurate. However, the number of scales of signal decomposed needs to select appropriately so that the information of the signal is preserved.

HT is a technique used to obtain the instantaneous frequencies and amplitude for the non-stationary signal [130]. A signal is decomposed into Intrinsic Mode Function (IMF) using the Empirical Mode Decomposition (EMD), which is a finite set of intrinsic components. The HT is applied to each IMFs to obtain the features of instantaneous frequencies and amplitude of the signal. The features are presented in time-frequency representation (Hilbert spectrum) for each IMF. In detecting the crack in the stainless steel pipe, the HT approach is used to decompose the signals obtained using the microwave guided wave technique [125]. The HT is applied to the IMFs for the detection of defects. The results present a high accuracy in defect detection as the noises and irrelevant signals are reduced. However, there are still some outliers in the interpretations. Besides, the application of EMD to break the beam down into IMFs causes the mode mixing problem for the signal.

Variational Mode Decomposition (VMD) technique can eradicate the mode mingling issue of EMD in decomposition by adopting the Alternate Direction Method Of Multipliers (ADMM) approach [126]. The VMD technique demonstrates its supremacy for predicting crude oil, wind velocity and image processing [131], [132]. VMD is a technique used to define a signal set of Variational Mode Functions (VMFs) and disintegrate the signal's fundamental modes around their respective predicted center frequencies. In other words, it can reduce the frequency overlapping among different intrinsic modes and signal complexity. In detecting the defects in the wind turbine gearbox and bearing, the vibration signal is split using the VMD technique [126]. The results demonstrate that VMD's reconstructed signals show significant results in defects' information. However, the mode number of the VMD technique needs to be pre-determined to avoid over and under decomposition problems.

A comparison between several preprocessing techniques is provided in Table 3. All the above-mentioned preprocessing techniques help to estimate defect detection more accurately. The HT and VMD techniques are suggested to combine since both of the techniques are working on the vibrating signals. In addition, the VMD technique can minimize the issue of mode mixing in the EMD technique. The VMD technique can replace the EMD technique to decompose signals into VMFs.

TABLE 3. Comparison summary of preprocessing techniques.

Ref. No.	Technique	Concept of use	Advantages	Disadvantages
[124]	DWT	Noise suspension from GW ultrasonic signals	- Signal noise can be removed. - Estimation of defect detection is accurate.	- Require selecting the number of scales of signal decomposed appropriately.
[125]	HT	Signal decomposition from ultrasonic sensors	- Increase the accuracy of defect detection.	- Outlier presence. - EMD causes mode mixing problem in signals decomposition.
[126]	VMD	Vibration signal decomposition from wind turbine gearbox and bearing	- Eliminate mode mixing problem in EMD technique. - Reduce the frequency overlapping among different intrinsic modes. - Reduce signal complexity.	- Performance depends on mode number. - Mode number needs to be pre-determined to avoid over and under decomposition problem.

Then, to acquire the features of instantaneous frequencies and amplitude of the signal, the HT approach is adopted for the VMFs. This can further increase the accuracy of defect detection.

B. FEATURE EXTRACTION

Feature extraction is a process to reduce data dimensionality to more manageable sets for data analysis [133]. In feature extraction, a selection process aims to obtain the dominant information and remove the redundant raw data factors. These redundant features reduce the predictive model's precision and agility, causing a significant impact on the model's analytical precision and implementation efficiency. In microwave NDT, the frequency sweeping generates a high dimensionality feature vector. This high dimensionality of the features increases the processing time and computational complexity of machine learning algorithms. Therefore, Partial Least Squares (PLS), Principal Component Analysis (PCA) and Nonnegative Matrix Factorization (NMF) are discussed in this section due to performing feature extraction and dimensionality reduction simultaneously.

PLS algorithm is one of the famous approaches to implementing feature extraction. PLS is a multivariate linear approach for analyzing the relations between two groups of variables which are dependent and independent [134]. The independent variables (predictors) scales, which reflect their linear combinations, are reduced to several Latent Variables (LVs). LVs eliminate the model's complexity by allocating X-space variables with no relationship to Y-space variables with low weights, lowering model overfit possibilities and increasing interpretability. To facilitate this, the orthogonal score PLS, referred to as the Non-Linear Estimation By Iterative Partial Least Squares (NIPALS) algorithm, boosts both the disparity and the regression with the response variables inside the predictors themselves. PLS can be implemented in regression, classification, variable selection, and survival analysis.

Ser. *et al.* [135] suggest the forecast of anti-corrosion performance, employing the Genetic Algorithm-Partial Least Square (GA-PLS) approach. The authors optimize the quantity of LVs utilized in the concept. They find out that three LVs exhibit the lowest Percentage Root Mean Square Error Of Cross-Validation (%RMSECV). The forecast of the GA-PLS model can be seen in the publication. From the graph, the authors conclude that the GA-PLS model is fairly successful, with some of the points not well scattered along with the parameters determined. Thus, the GA-PLS model reveals that the correlations between the quantum chemical factors and inhibitor performance are not effectively captured.

PCA algorithm is one of the methods used to perform feature extraction. PCA is commonly used to reduce high-dimensional data to low-dimensional data [136]. It substitutes a smaller number of uncorrelated principal components for a large number of original interrelated variables while retaining the information in the data set of original variables. PCA is well-known for identifying analytical patterns with massive data volumes [137]. Besides that, PCA is a uniform conversion of data into a new reference frame to position the axis with the greatest variance becoming the primary significant element and the following largest part as the second principal component when the data is mapped to one axis.

Ali *et al.* [138] propose a Supervised-PCA (SPCA) technique in their paper to image the CUI in metallic structures. The authors show the SPCA 2D visualization in their paper. SPCA technique is used to project the explicative variables according to the direction of the response variables. PCA maps the periodicity points to 15 dominant components in lower frequency. SPCA is applied to the training and test data sets. An outstanding result is obtained in this paper. The SPCA succeeds in extracting and differentiating the information with corrosion and without corrosion. Then, the ML algorithm is applied to classify the inspected locations into corrosion and corrosion-free over a 2D spatial image. This shows good applicability of undetected flaws in terms of fault pattern classification and sharp lateral resolutions. However, the lower frequency characteristics do not correlate to the sweeping frequencies as the disappearance of initial data.

NMF algorithm is implemented for feature extraction in dimension reduction [139]. The NMF algorithm is a

collection of algorithms for multivariate analysis and linear algebra. A low-rank matrix approximation is used by NMF to approximate a matrix [140]. In other words, when the original high-dimensional data matrix is recreated using solely additive linear combinations, it is transformed into a data representation based on parts [141], [142]. NMF is a typical technique for segregating spatial frequency characteristics blindly into defect and defect-free regions.

The smooth Itakura-Saito NMF (S-ISNMF) algorithm is suggested by Gao *et al.* [143] for the detection of CUI in a coated steel pipeline using an X-band OERW approach. S-ISNMF algorithm is used for the purpose of analyzing the frequency spectrum characteristics of the reflected signals between defect and defect-free areas. Location and shape estimation of the CUI are both effectively accomplished using the S-ISNMF algorithm. The smoothness parameter contributed to the improvement of the sensitivity of the microwave NDT system while simultaneously reducing noise. The S-ISNMF algorithm estimates the defects' shape with 82.6 % accuracy. However, as a consequence of these varying beginning optimization parameters, NMF yields a different estimated outcome at each iteration of the program. [30]. Additionally, when the spectral resolution is poor, NMF delivers the worst results [144].

Table 4 shows the comparison between the PLS, PCA and NMF algorithms. The PLS algorithm can be employed with the genetic algorithm. The number of LVs used is optimized by using GA-PLS. Besides that, it exhibits the lowest %RMSECV. It is quite efficient for simple processes. For PCA algorithm, it can be utilized to become a supervised-PCA approach. It can project explicative variables according to the direction of the response variables. It is successfully extracted and differentiates the information with corrosion and without corrosion. Supervised-PCA is very efficient for simple processes. However, two approaches can be regarded as low learning approaches with one hidden layer model structure. They can be efficient for simple processes, but their expressive capacity for complex structures can be inadequate [137]. For the NMF algorithm, it is very efficient for CUI shape and location estimation as the NMF algorithm successfully estimates the CUI shape with 82.6 % accuracy. However, the NMF algorithm provides a different approximated result for each run time. Hence, the feature extraction algorithm must collaborate with the feature classification algorithm to obtain a better prediction result.

C. CLASSIFICATION STAGE

In the classification stage, a classifier algorithm is used to split a set of observations into subset groups according to their type. There are two categories for data classification: Supervised Machine Learning (SML) algorithms and unsupervised machine learning algorithms. Supervised learning provides a function to map inputs to desired outputs [145]. Such approaches require prior status labeling in renowned regimes (i.e., input data). Figure 8 illustrates the process of SML. For unsupervised learning, it learns structure from the

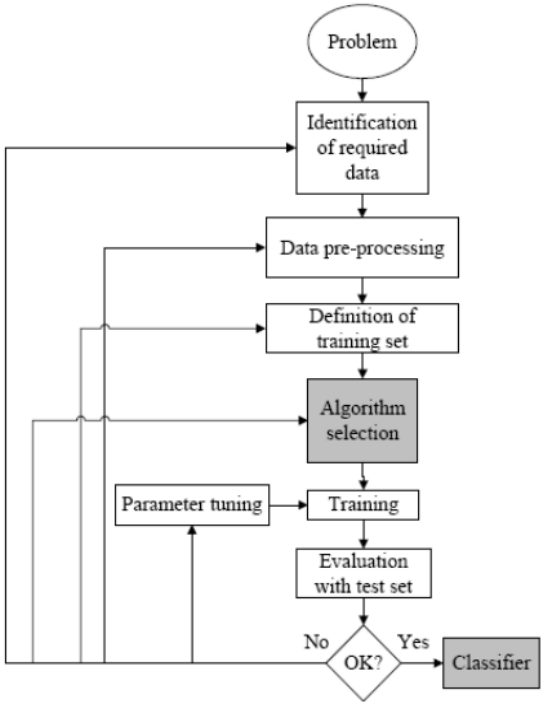

FIGURE 8. Supervised machine learning (SML) process [145].

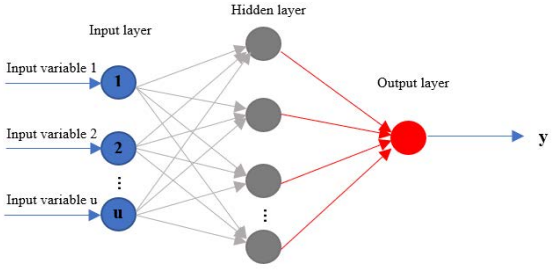

FIGURE 9. Typical artificial neural network architecture.

data without prior labeling. Unsupervised learning is useful once the prior knowledge is not available or the sample size is small [147].

Artificial Neural Network (ANN) is one of the SML algorithms. ANN model is an essential tool for addressing complicated issues [148]. The imaginary network feeds information from the information source to the initial level's neural neurons. The neurons convert the data into an impulse and transmit the impulse to the neurons in the following tier as an input. The precision with which the results were produced improves as the neural network learns. The neural networks make a decision based on prior learning and extrapolate from them. Figure 9 demonstrates the architecture of a typical ANN.

Analyses of the ANN ensemble are presented by Ali *et al.* [149]. The authors adopt a waveguide sensor equipped with split-ring resonators-based ANN to improve the defect detection accuracy. ANN and Support Vector Machine (SVM)

TABLE 4. Comparison summary of the feature extraction approaches.

Ref. No.	Technique	Concept of use	Advantages	Disadvantages
[135]	PLS	GA-PLS in forecasting the anti-corrosion performance	- Number of LVs used is optimised. - Lowest %RMSECV. - Efficient for simple processes.	- Low learning approach. - One hidden layer model structure. - Inadequate for complex structures.
[138]	PCA	Supervised-PCA in imaging the CUI	- Project explicative variables according to the direction of the response variables. - Succeed to extract and differentiate the information with corrosion and without corrosion. - Efficient for simple processes.	- Lower frequency characteristics do not correlate to the sweeping frequencies. - Inadequate for complex structures.
[143]	NMF	S-ISNMF in CUI detection	- Succeed to detect the CUI in terms of location and shape estimation. - 82.6 % accuracy of defects' shape estimation.	- Different approximated result for each run time. - Worst result when low spectral resolution.

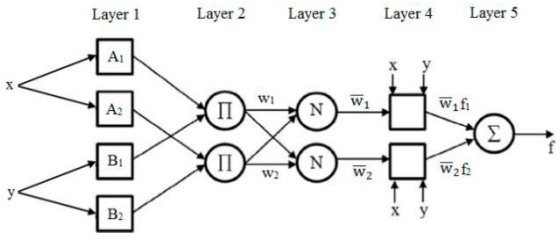

FIGURE 10. The architecture of ANFIS technique [146].

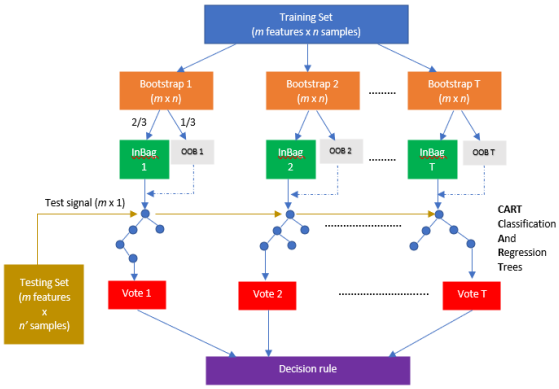

FIGURE 11. Workflow of the random forests (RF) algorithm.

classifiers are integrated to create a hybrid AI model. The combined model has a defect classification accuracy of 99.62 %. Adaptive Neural Based Fuzzy Inference System (ANFIS) is used to enhance the prediction of corrosion rate by lessening the dependency on data as ANFIS can simulate the existing data while accounting for expertise's insights [150]. ANFIS is an adaptive system employing the ANN and Fuzzy Logic (FL). The authors present the analysis of the ANFIS model in CUI in their paper. Figure 10 shows the architecture of the ANFIS technique with two sources, one outcome and two criteria [146]. It can be employed to evaluate the degree of CUI. This model shows a successful result in predicting the corrosion rate as it is only a 0.0005 Mean Absolute Deviation (MAD) value. ANFIS model enhances the corrosion rate prediction by taking into account the all the input parameters for the cause of CUI, such as insulation condition, type of insulation and environment. Moreover, there is an additional benefit of the ability to observe the level of degradation at each temperature. However, the parameters of the ANFIS model (center and spread of each membership function) need to be pre-determined to avoid prediction error.

Random Forests (RF) is used to predict and make a decision by dividing the original data randomly. RF is a supervised classification based on an ensemble learning approach. RF works with the theory of establishing a multiplicity of decision trees throughout the learning process, where each of them can produce a reaction if a new collection of elements is presented while screening [151]. Breiman's "bagging" and spontaneous partition of elements are combined in this approach to create a regulated variance decision tree series. Figure 11 presents the workflow of the RF algorithm. The networks are randomly distributed via bootstrap clustering, with every tree being built on a randomly chosen labeled dataset and split classification.

Microwave NDT-based RF defect classification was proposed by Pan *et al.* [152] in their publication. Microwave ground penetrating radar is used in this research to detect the defect. The RF algorithm is then employed to classify the defects. Defects are classified with a precision of 98 % using the RF algorithm. The RF algorithm, in addition, reduces the amount of time required to complete the defect categorization process. In order to identify additional defect mechanisms, it is recommended that the learning library be expanded.

The supervised ML algorithms are efficient and powerful as they can solve complex problems and provide high accuracy on the corrosion rate, size and depth of the inspected area. However, SML algorithms require a pre-knowledge, such as training sample labeling to learn before they predict the CUI with high precision. Compared to supervised

TABLE 5. Comparison summary of the feature classification approaches.

Ref. No.	Technique	Concept of use	Advantages	Disadvantages
[149]	ANN-waveguide sensor with split-ring resonators	ANN ensemble for defect assessment	- 99.62 % accuracy of defect classification.	- No defect evaluation.
[152]	RF-microwave GPR	Defect classification	- 98 % accuracy in classifying the defects.	- Learning library is required to be larger.
[153]	K-means	Traditional K-means in the Hue component	- Sufficient to detect rust with images of H% higher than 98%. - Suitable for image recognition and clustering.	- Prediction accuracy reduces when the images are non-red bridges.
[50]	K-means based IFFT	Defect detection in steel pipeline coated with GFRP	- Small-size defects are significantly detected.	- Sensitive to outlier presence which degrades the clustering accuracy. - Fail to deal with overlapping clusters
[154]	FCM-OEWA	Defect detection and visualization	- Microwave poor resolution images are improved. - Area of interest is identified.	- Sensitive to noise and outliers.
[155]	GMM	Membership determination for open clusters	- Provide the details of mean and covariance. - Optimize the probability estimation of distribution parameters. - Fast model with a runtime complexity. - Possible for each cluster to describe data points.	- Require high-precision data collection. - Require a high percentage of cluster members. - Require various locations in the peak of field star and cluster member distribution.

approaches, unsupervised ML algorithms aid the analysis of input data sources, assisting in generating empirical findings from unlabeled inputs without the need for prior labeling.

K-means clustering algorithm is one of the basic unsupervised learning algorithms employed to address the grouping issue. The k-means algorithm splits the collected data into k of clusters. The data within each cluster is quite similar and different from other clusters. The k-means algorithm is utilized once the data labeling is not provided for the training set. Liao *et al.* [153] recommended the traditional K-means technique in the Hue (H) component to identify corrosion issues on the steel bridge coatings using digital image identification. They observed that the conventional K-means algorithm in the H portion is sufficient to detect rust with the images with H% higher than 98%, known as group A. The observation proves that K-means is very suitable for image recognition and clustering algorithms.

The K-means clustering algorithm is used with a microwave NDT technique to boost the image analysis performance and flaw discovery in composite materials [50]. The reflection coefficient of the microwave signals is obtained from Glass Fiber Reinforced Polymer (GFRP) using the OERW probe. Inverse Fast Fourier Transform (IFFT) is employed to translate the reflection coefficients to the time domain. Thereafter, the magnitude of the converted data is clustered into two groups which are defect and defect-free. The proposed technique significantly detects small-size defects compared to several conventional microwave NDT techniques. However, the extent of delamination is larger than the actual one as the outlier presence in microwave reflection coefficients. In addition, the k-means algorithm assigns the objects exclusively to one cluster and fails to deal with overlapping clusters [156].

It is possible to allocate objects to numerous groups using the Fuzzy C-Means (FCM) clustering algorithm and to cope with overlapping clusters [157]. The FCM algorithm splits objects into clusters based on their greatest similarities, whereas the least similar objects are divided into distinct clusters [158]. Hoshyar *et al.* [154] proposed a microwave NDT-based FCM clustering algorithm for defect identification and visualization. The Open-Ended Waveguide Antenna (OEWA) is used for defect detection in composite material-coated metal discs. The findings show that the FCM algorithm is able to accurately identify and depict the issue. The low-resolution microwave images are effectively improved using FCM, allowing it to locate the defects' locations. FCM, on the other hand, continues to make mistakes by incorrectly classifying certain regions that are not defective as defective zones. This is due to the fact that FCM is very sensitive to outliers and noise.

Compared to FCM, Gaussian Mixture Model (GMM) is less influenced by the outliers. GMM is a stochastic framework in which all information is taken from a collection of Gaussian distribution with uncertain variables [155]. GMM can be known as the outgrowth algorithm of K-means clustering as GMM provides details about the mean and the covariance, which defines a distribution's ellipsoidal shape. The expectation-maximization algorithm is used to suit the

GMM by optimizing the probability estimates of distribution parameters.

Table 5 presents the comparison of machine learning-based microwave NDT techniques. The feature classification is used to enhance the prediction of defect detection by minimizing the prediction error of the prediction factor. It lessens the dependency on the data. It is very suitable for image recognition and clustering. The inspection quality in terms of defect detection, classification, size, depth and shape is further improved compared to the conventional techniques. Moreover, the prospect of using ML algorithms that are used with conventional NDT is also applicable to microwave NDT. There are still more works to be done in researching the ML-based microwave NDT approach to add more advantages in inspecting CUI.

Based on our knowledge, there is no corrosion inspection research has yet been done on this algorithm. GMM can offer many advantages for the inspection of corrosion. GMM is a very fast model with a runtime complexity. In addition, GMM is possible for each cluster to describe the data point. High-precision data collection, a high percentage of cluster members, and various locations in the peak of field star and cluster member distribution are, however, needed. With the reliability of the membership determination and classification, GMM will do well in the CUI inspection.

V. CONCLUSION

Conventional NDT techniques are incredibly essential in industrial and service. These techniques can predict the CUI earlier without removing the insulation layer before catastrophic damage occurs. The performance of the inspection of CUI using conventional NDT techniques, which are profile radiography, infrared thermography, scanning Kelvin Probe, ultrasonic testing, and eddy current testing, is degraded as the development of composite materials become the insulation layer of the metal. This is because of the field penetration limitation of conventional NDT techniques in composite materials. In addition, the conventional NDT techniques face the spatial figure with low sharpness and fuzzy defect pattern challenges. Using the microwave NDT technique, the microwave signals can penetrate the insulation layer and detect the CUI. Moreover, the microwave NDT techniques provide non-contact, operator-friendly processing, no couplant and no complicated post-processing over conventional NDT techniques. Thus, the trend of using microwave NDT techniques has risen among researchers and in the industries. However, these great techniques are still facing some challenges, such as stand-off deviations and appropriate frequency points to be chosen, which will reduce the quality of inspection of CUI.

Among all the microwave NDT techniques, rectangular waveguides show better performance in the inspection of CUI. The rectangular waveguide can perform on its own or collaborate with other components. However, the detection of the whole area of corrosion is still a limitation of rectangular waveguides. This is because the researchers focus on enhancing the quality of sensors while lacking soft computing techniques applied in microwave NDT techniques. The outliers can be removed by soft computing approaches to improve the accuracy of detected CUI.

Soft computing methods like signal processing and artificial intelligence-based machine learning can solve noise in the signal and signal complexity. Therefore, the soft computing techniques can collaborate with microwave NDT techniques to solve the limitations and achieve a positive result for the inspection of CUI. As mentioned, materials inspection using microwave NDT techniques might cause default-free diffraction on the edges of the defect. By using the machine learning technique, it is possible to identify the defect and non-defect areas as it can solve complex and non-linear data.

In addition, AI-based machine learning techniques can be used to detect and image the severity of the CUI. Besides that, they can provide the prediction on the CUI and estimate the remaining life of the material under test. Hence, early preparation can be done by the industrial to repair or change the materials under test. The application of deep learning in microwave NDT techniques can also build an automated mechanism for enhancing the effectiveness and control of products during manufacturing and operation.

REFERENCES

[1] Q. Cao, M. Brameld, N. Birbilis, and S. Thomas, "On the mitigation of corrosion under insulation (CUI) of mild steel using local cathodic protection," *Corrosion*, vol. 75, no. 12, pp. 1541–1551, Dec. 2019, doi: 10.5006/3197.

[2] N. R. A. Burhani, M. Muhammad, and M. C. Ismail, "Corrosion under insulation rate prediction model for piping by two stages of artificial neural network," in *Proc. AIP Conf.*, vol. 2035, no. 1, 2018, Art. no. 030004, doi: 10.1063/1.5075560.

[3] B. Bavarian, Y. Ikder, B. Samimi, and L. Reiner, "Protection of corrosion under insulation using vapor phase corrosion inhibitors, corrologic V_pCI-658," Cortec Corp., Saint Paul, MN, USA, Apr. 2015. Accessed: Mar. 1, 2022. [Online]. Available: https://www.cortecvci.com/Publications/Papers/Corrologic-VpCI-658-inhibitor-effects-on-CUI-final-report.pdf

[4] Y.-H. Tsai, J. Wang, W.-T. Chien, C.-Y. Wei, X. Wang, and S.-H. Hsieh, "A BIM-based approach for predicting corrosion under insulation," *Autom. Construct.*, vol. 107, Nov. 2019, Art. no. 102923, doi: 10.1016/j.autcon.2019.102923.

[5] E. O. Eltai, F. Musharavati, and E. S. Mahdi, "Severity of corrosion under insulation (CUI) to structures and strategies to detect it," *Corrosion Rev.*, vol. 37, no. 6, pp. 553–564, Dec. 2019, doi: 10.1515/corrrev-2018-0102.

[6] M. F. Akbar, N. H. M. M. Shrifan, G. N. Jawad, and N. A. M. Isa, "Assessment of delamination under insulation using ridge waveguide," *IEEE Access*, vol. 10, pp. 36177–36187, 2022, doi: 10.1109/ACCESS.2022.3163308.

[7] Z. Yuan, Y. Tu, Y. Zhao, H. Jiang, and C. Wang, "Degradation behavior and aging mechanism of decay-like fractured GRP rod in composite insulator," *IEEE Trans. Dielectr. Electr. Insul.*, vol. 26, no. 3, pp. 1027–1034, Jun. 2019, doi: 10.1109/TDEI.2019.007788.

[8] W. Tu, S. Zhong, Y. Shen, and A. Incecik, "Nondestructive testing of marine protective coatings using terahertz waves with stationary wavelet transform," *Ocean Eng.*, vol. 111, pp. 582–592, Jan. 2016, doi: 10.1016/j.oceaneng.2015.11.028.

[9] R. Yang, Y. He, H. Zhang, and S. Huang, "Through coating imaging and nondestructive visualization evaluation of early marine corrosion using electromagnetic induction thermography," *Ocean Eng.*, vol. 147, pp. 277–288, Jan. 2018, doi: 10.1016/j.oceaneng.2017.09.023.

[10] M. J. Cullin, G. Birmingham, R. Srinivasan, and G. Hailu, "Injectable sodium bentonite inhibitors for corrosion under insulation," *J. Pipeline Syst. Eng. Pract.*, vol. 11, no. 4, Jun. 2020, Art. no. 04020036, doi: 10.1061/(asce)ps.1949-1204.0000488.

[11] M. Yang and J. Liu, "*In situ* monitoring of corrosion under insulation using electrochemical and mass loss measurements," *Int. J. Corrosion*, vol. 2022, pp. 1–12, Jan. 2022, doi: 10.1155/2022/6681008.
[12] S. Winnik, "Corrosion-under-insulation (CUI) guidelines revised edition," in *Europaen Federation of Corrosion*, vol. 55. Cambridge, U.K.: Woodhead Publishing, 2016, pp. 67–70.
[13] J. Z. Yi, H. X. Hu, Z. B. Wang, and Y. G. Zheng, "Comparison of critical flow velocity for erosion-corrosion of six stainless steels in 3.5 wt% NaCl solution containing 2 wt% silica sand particles," *Wear*, vols. 416–417, pp. 62–71, Dec. 2018, doi: 10.1016/j.wear.2018.10.006.
[14] S. K. Dwivedi, M. Vishwakarma, and P. A. Soni, "Advances and researches on non destructive testing: A review," *Mater. Today, Proc.*, vol. 5, no. 2, pp. 3690–3698, 2018, doi: 10.1016/j.matpr.2017.11.620.
[15] A. Hunze, J. Bailey, G. Sidorov, P. Bondurant, and T. Mactutis, "Non-destructive testing of critical infrastructure with giant magneto resistive sensors," *Proc. SPIE*, vol. 9804, pp. 319–328, Apr. 2016, doi: 10.1117/12.2217930.
[16] F. Varela, M. Yongjun Tan, and M. Forsyth, "An overview of major methods for inspecting and monitoring external corrosion of on-shore transportation pipelines," *Corrosion Eng., Sci. Technol.*, vol. 50, no. 3, pp. 226–235, May 2015, doi: 10.1179/1743278215Y.0000000013.
[17] F. Zou and F. B. Cegla, "On quantitative corrosion rate monitoring with ultrasound," *J. Electroanal. Chem.*, vol. 812, pp. 115–121, Mar. 2018, doi: 10.1016/j.jelechem.2018.02.005.
[18] M. F. Akbar, G. N. Jawad, L. R. Danoon, and R. Sloan, "Delamination detection in glass-fibre reinforced polymer (GFRP) using microwave time domain reflectometry," in *Proc. 15th Eur. Radar Conf. (EuRAD)*, Sep. 2018, pp. 253–256, doi: 10.23919/EURAD.2018.8546540.
[19] M. F. Akbar, "Delamination thickness estimation using microwave time domain reflectometry," in *Material Characterisation and Nondestructive Testing using Microwave Technique*. Manchester, U.K.: Univ. Manchester, 2018.
[20] H. Yang, Q. Chen, H. Cao, D. Fan, J. Huang, J. Zhao, B. Yan, W. Zhou, W. Zhang, and H. Zhang, "Radiofrequency thawing of frozen minced fish based on the dielectric response mechanism," *Innov. Food Sci. Emerg. Technol.*, vol. 52, pp. 80–88, Mar. 2019, doi: 10.1016/j.ifset.2018.10.013.
[21] R. Li, S. Zhang, X. Kou, B. Ling, and S. Wang, "Dielectric properties of almond kernels associated with radio frequency and microwave pasteurization," *Sci. Rep.*, vol. 7, no. 1, pp. 1–10, Feb. 2017, doi: 10.1038/srep42452.
[22] R. Wu, H. Zhang, R. Yang, W. Chen, and G. Chen, "Nondestructive testing for corrosion evaluation of metal under coating," *J. Sensors*, vol. 2021, pp. 1–16, Jun. 2021, doi: 10.1155/2021/6640406.
[23] C. Viegas, B. Alderman, P. G. Huggard, J. Powell, K. Parow-Souchon, M. Firdaus, H. Liu, C. I. Duff, and R. Sloan, "Active millimeter-wave radiometry for nondestructive testing/evaluation of composites—Glass fiber reinforced polymer," *IEEE Trans. Microw. Theory Techn.*, vol. 65, no. 2, pp. 641–650, Feb. 2017, doi: 10.1109/TMTT.2016.2625785.
[24] H. Zhang, Y. He, B. Gao, G. Y. Tian, L. Xu, and R. Wu, "Evaluation of atmospheric corrosion on coated steel using K-band sweep frequency microwave imaging," *IEEE Sensors J.*, vol. 16, no. 9, pp. 3025–3033, May 2016, doi: 10.1109/JSEN.2016.2522983.
[25] M. F. Akbar, G. N. Jawad, C. I. Duff, and R. Sloan, "Porosity evaluation of in-service thermal barrier coated turbine blades using a microwave nondestructive technique," *NDT E, Int.*, vol. 93, pp. 64–77, Jan. 2018, doi: 10.1016/j.ndteint.2017.09.015.
[26] N. H. M. M. Shrifan, M. F. Akbar, and N. A. M. Isa, "Prospect of using artificial intelligence for microwave nondestructive testing technique: A review," *IEEE Access*, vol. 7, pp. 110628–110650, 2019, doi: 10.1109/ACCESS.2019.2934143.
[27] T. W. Siang, M. Firdaus Akbar, G. Nihad Jawad, T. S. Yee, and M. I. S. M. Sazali, "A past, present, and prospective review on microwave nondestructive evaluation of composite coatings," *Coatings*, vol. 11, no. 8, p. 913, Jul. 2021, doi: 10.3390/coatings11080913.
[28] M. Yi, S. Li, H. Yu, W. Khan, C. Ulusoy, A. Vera-Lopez, J. Papapolymerou, and M. Swaminathan, "Surface roughness modeling of substrate integrated waveguide in D-band," *IEEE Trans. Microw. Theory Techn.*, vol. 64, no. 4, pp. 1209–1216, Apr. 2016, doi: 10.1109/TMTT.2016.2535290.
[29] K. Lomakin, G. Gold, and K. Helmreich, "Analytical waveguide model precisely predicting loss and delay including surface roughness," *IEEE Trans. Microw. Theory Techn.*, vol. 66, no. 6, pp. 2649–2662, Jun. 2018, doi: 10.1109/TMTT.2018.2827383.
[30] N. H. M. M. Shrifan, M. F. Akbar, and N. A. M. Isa, "Maximal overlap discrete wavelet-packet transform aided microwave nondestructive testing," *NDT E, Int.*, vol. 119, Apr. 2021, Art. no. 102414, doi: 10.1016/j.ndteint.2021.102414.
[31] P. Asadi, M. Gindy, and M. Alvarez, "A machine learning based approach for automatic rebar detection and quantification of deterioration in concrete bridge deck ground penetrating radar B-scan images," *KSCE J. Civil Eng.*, vol. 23, no. 6, pp. 2618–2627, Jun. 2019, doi: 10.1007/s12205-019-2012-Z.
[32] M. S. Coutinho, L. R. G. S. Lourenço Novo, M. T. De Melo, L. H. A. De Medeiros, D. C. P. Barbosa, M. M. Alves, V. L. Tarragô, R. G. M. Dos Santos, H. B. T. D. L. Neto, and P. H. R. P. Gama, "Machine learning-based system for fault detection on anchor rods of cable-stayed power transmission towers," *Electric Power Syst. Res.*, vol. 194, May 2021, Art. no. 107106, doi: 10.1016/j.epsr.2021.107106.
[33] N. H. M. M. Shrifan, M. F. Akbar, and N. A. M. Isa, "An adaptive outlier removal aided k-means clustering algorithm," *J. King Saud Univ.-Comput. Inf. Sci.*, pp. 1–12, Jul. 2021, doi: 10.1016/J.JKSUCI.2021.07.003.
[34] M. Alber, A. B. Tepole, W. R. Cannon, S. De, S. Dura-Bernal, K. Garikipati, G. Karniadakis, W. W. Lytton, P. Perdikaris, L. Petzold, and E. Kuhl, "Integrating machine learning and multiscale modeling—Perspectives, challenges, and opportunities in the biological, biomedical, and behavioral sciences," *NPJ Digit. Med.*, vol. 2, no. 1, pp. 1–11, Nov. 2019, doi: 10.1038/s41746-019-0193-y.
[35] B. Mirza, W. Wang, J. Wang, H. Choi, N. C. Chung, and P. Ping, "Machine learning and integrative analysis of biomedical big data," *Genes*, vol. 10, no. 2, p. 87, Jan. 2019, doi: 10.3390/genes10020087.
[36] H. Seo, M. B. Khuzani, V. Vasudevan, C. Huang, H. Ren, R. Xiao, X. Jia, and L. Xing, "Machine learning techniques for biomedical image segmentation: An overview of technical aspects and introduction to state-of-art applications," *Med. Phys.*, vol. 47, no. 5, pp. e148–e167, May 2020, doi: 10.1002/mp.13649.
[37] W. Luo, D. Phung, T. Tran, S. Gupta, S. Rana, C. Karmakar, A. Shilton, J. Yearwood, N. Dimitrova, T. B. Ho, S. Venkatesh, and M. Berk, "Guidelines for developing and reporting machine learning predictive models in biomedical research: A multidisciplinary view," *J. Med. Internet Res.*, vol. 18, no. 12, p. e323, Dec. 2016, doi: 10.2196/jmir.5870.
[38] J. Rodellar, S. Alférez, A. Acevedo, A. Molina, and A. Merino, "Image processing and machine learning in the morphological analysis of blood cells," *Int. J. Lab. Hematol.*, vol. 40, pp. 46–53, May 2018, doi: 10.1111/ijlh.12818.
[39] Z. Wang, H. Di, M. A. Shafiq, Y. Alaudah, and G. Alregib, "Successful leveraging of image processing and machine learning in seismic structural interpretation: A review," *Leading Edge*, vol. 1, vol. 37, no. 6, pp. 451–461, Jun. 2018, doi: 10.1190/tle37060451.1.
[40] H. Singh, *Practical Machine Learning and Image Processing*. Berkeley, CA, USA: Apress, 2019, pp. 1–169, doi: 10.1007/978-1-4842-4149-3.
[41] A. Le Glaz, Y. Haralambous, D.-H. Kim-Dufor, P. Lenca, R. Billot, T. C. Ryan, J. Marsh, J. DeVylder, M. Walter, S. Berrouiguet, and C. Lemey, "Machine learning and natural language processing in mental health: Systematic review," *J. Med. Internet Res.*, vol. 23, no. 5, May 2021, Art. no. e15708, doi: 10.2196/15708.
[42] M. Khanbhai, P. Anyadi, J. Symons, K. Flott, A. Darzi, and E. Mayer, "Applying natural language processing and machine learning techniques to patient experience feedback: A systematic review," *BMJ Health Care Informat.*, vol. 28, no. 1, Mar. 2021, Art. no. 100262, doi: 10.1136/bmjhci-2020-100262.
[43] S. L. Marie-Sainte, N. Alalyani, S. Alotaibi, S. Ghouzali, and I. Abunadi, "Arabic natural language processing and machine learning-based systems," *IEEE Access*, vol. 7, pp. 7011–7020, 2019, doi: 10.1109/ACCESS.2018.2890076.
[44] A. Niccolai, D. Caputo, L. Chieco, F. Grimaccia, and M. Mussetta, "Machine learning-based detection technique for NDT in industrial manufacturing," *Mathematics*, vol. 9, no. 11, p. 1251, May 2021, doi: 10.3390/math9111251.
[45] J. B. Harley and D. Sparkman, "Machine learning and NDE: Past, present, and future," in *Proc. AIP Conf.*, 2019, Art. no. 090001, doi: 10.1063/1.5099819.
[46] I. Virkkunen, T. Koskinen, O. Jessen-Juhler, and J. Rinta-aho, "Augmented ultrasonic data for machine learning," *J. Nondestruct. Eval.*, vol. 40, no. 1, pp. 1–11, Mar. 2021, doi: 10.1007/s10921-020-00739-5.
[47] K. Ikeda and A. Kamimura, "Hammering acoustic analysis using machine learning techniques for piping inspection," *J. Robot. Mechtron.*, vol. 32, no. 4, pp. 789–797, Aug. 2020, doi: 10.20965/jrm.2020.p0789.

[48] M. F. Sheikh, K. Kamal, F. Rafique, S. Sabir, H. Zaheer, and K. Khan, "Corrosion detection and severity level prediction using acoustic emission and machine learning based approach," *Ain Shams Eng. J.*, vol. 12, no. 4, pp. 3891–3903, Dec. 2021, doi: 10.1016/j.asej.2021.03.024.

[49] A. Amer, A. Alshehri, H. Saiari, A. Meshaikhis, and A. Alshamrany, "Artificial intelligence AI assisted thermography to detect corrosion under insulation CUI," in *Proc. SPE Middle East Oil Gas Show Conf.*, Dec. 2021, doi: 10.2118/204690-MS.

[50] N. H. M. M. Shrifan, G. N. Jawad, N. A. M. Isa, and M. F. Akbar, "Microwave nondestructive testing for defect detection in composites based on K-means clustering algorithm," *IEEE Access*, vol. 9, pp. 4820–4828, 2021, doi: 10.1109/ACCESS.2020.3048147.

[51] M. Grenier, V. Demers-Carpentier, M. Rochette, and F. Hardy, "Pulsed eddy current: New developments for corrosion under insulation examinations," in *Proc. 19th World Conf. Non-Destructive Test.*, 2016, pp. 13–17. Accessed: Mar. 12, 2022. [Online]. Available: http://ndt.net/?id=19239

[52] A. Amer, S. Aramco, A. Alshehri, and I. Al-Taie, "Inspection challenges for detecting corrosion under insulation (CUI) in the oil and gas industry," in *Proc. 17th Middle East Corrosion Conf. Exhib.*, 2018, pp. 1–4.

[53] M. Jolly, A. Prabhakar, B. Sturzu, K. Hollstein, R. Singh, S. Thomas, P. Foote, and A. Shaw, "Review of non-destructive testing (NDT) techniques and their applicability to thick walled composites," *Proc. CIRP*, vol. 38, pp. 129–136, Jan. 2015, doi: 10.1016/j.procir.2015.07.043.

[54] M. Margret, M. Menaka, V. Subramanian, R. Baskaran, and B. Venkatraman, "Non-destructive inspection of hidden corrosion through Compton backscattering technique," *Radiat. Phys. Chem.*, vol. 152, pp. 158–164, Nov. 2018, doi: 10.1016/j.radphyschem.2018.07.015.

[55] S. Doshvarpassand, C. Wu, and X. Wang, "An overview of corrosion defect characterization using active infrared thermography," *Infr. Phys. Technol.*, vol. 96, pp. 366–389, Jan. 2019, doi: 10.1016/J.INFRARED.2018.12.006.

[56] S. Varvara, C. Berghian-Grosan, R. Bostan, R. L. Ciceo, Z. Salarvand, M. Talebian, K. Raeissi, J. Izquierdo, and R. M. Souto, "Experimental characterization, machine learning analysis and computational modelling of the high effective inhibition of copper corrosion by 5-(4-pyridyl)-1,3,4-oxadiazole-2-thiol in saline environment," *Electrochimica Acta*, vol. 398, Dec. 2021, Art. no. 139282, doi: 10.1016/j.electacta.2021.139282.

[57] M. Dorfer, R. Kelz, and G. Widmer, "Deep linear discriminant analysis," in *Proc. Int. Conf. Learn. Representations*, 2016, pp. 1–13. Accessed: Apr. 4, 2022. [Online]. Available: http://www.cp.jku.at/

[58] A. Tharwat, T. Gaber, A. Ibrahim, and A. E. Hassanien, "Linear discriminant analysis: A detailed tutorial," *AI Commun.*, vol. 30, no. 2, pp. 169–190, Jan. 2017, doi: 10.3233/AIC-170729.

[59] D. S. Herd, "Microwave based monitoring system for corrosion under insulation," Heriot-Watt Univ., Edinburgh, AS, U.K., Tech. Rep., 2016.

[60] M. Wicker, B. P. Alduse, and S. Jung, "Detection of hidden corrosion in metal roofing shingles utilizing infrared thermography," *J. Building Eng.*, vol. 20, pp. 201–207, Nov. 2018, doi: 10.1016/j.jobe.2018.07.018.

[61] F. Ciampa, P. Mahmoodi, F. Pinto, and M. Meo, "Recent advances in active infrared thermography for non-destructive testing of aerospace components," *Sensors*, vol. 18, no. 2, p. 609, Feb. 2018, doi: 10.3390/s18020609.

[62] G. Cadelano *et al.*, "Corrosion detection in pipelines using infrared thermography: Experiments and data processing methods," *J. Nondestruct. Eval.*, vol. 35, no. 49, pp. 1–11, Aug. 2016, doi: 10.1007/S10921-016-0365-5.

[63] M. Grosso, I. C. P. Margarit-Mattos, and G. R. Pereira, "Pulsed thermography inspection of composite anticorrosive coatings: Defect detection and analysis of their thermal behavior through computational simulation," *Materials*, vol. 13, no. 21, p. 4812, Oct. 2020, doi: 10.3390/ma13214812.

[64] C. Liu and R. G. Kelly, "A review of the application of finite element method (FEM) to localized corrosion modeling," *Corrosion*, vol. 75, no. 11, pp. 1285–1299, Nov. 2019, doi: 10.5006/3282.

[65] Q. Fang, C. Ibarra-Castanedo, and X. Maldague, "Automatic defects segmentation and identification by deep learning algorithm with pulsed thermography: Synthetic and experimental data," *Big Data Cognit. Comput.*, vol. 5, no. 1, p. 9, Feb. 2021, doi: 10.3390/bdcc5010009.

[66] A. A. Heidari, H. Faris, S. Mirjalili, I. Aljarah, and M. Mafarja, "Ant lion optimizer: Theory, literature review, and application in multi-layer perceptron neural networks," *Nature-Inspired Optimizers* (Studies in Computational Intelligence), vol. 811. 2020, pp. 23–46, doi: 10.1007/978-3-030-12127-3_3.

[67] A. A. Heidari, H. Faris, I. Aljarah, and S. Mirjalili, "An efficient hybrid multilayer perceptron neural network with grasshopper optimization," *Soft Comput.*, vol. 23, no. 17, pp. 7941–7958, Jul. 2018, doi: 10.1007/s00500-018-3424-2.

[68] Z. Zhao, S. Xu, B. H. Kang, M. M. J. Kabir, Y. Liu, and R. Wasinger, "Investigation and improvement of multi-layer perceptron neural networks for credit scoring," *Exp. Syst. Appl.*, vol. 42, no. 7, pp. 3508–3516, May 2015, doi: 10.1016/j.eswa.2014.12.006.

[69] Y. Cao, Y. Dong, Y. Cao, J. Yang, and M. Y. Yang, "Two-stream convolutional neural network for non-destructive subsurface defect detection via similarity comparison of lock-in thermography signals," *NDT E, Int.*, vol. 112, Jun. 2020, Art. no. 102246, doi: 10.1016/j.ndteint.2020.102246.

[70] A. N. AbdAlla, M. A. Faraj, F. Samsuri, D. Rifai, K. Ali, and Y. Al-Douri, "Challenges in improving the performance of eddy current testing: Review," *Meas. Control*, vol. 52, nos. 1–2, pp. 46–64, Nov. 2018, doi: 10.1177/0020294018801382.

[71] L. Xie, B. Gao, G. Y. Tian, J. Tan, B. Feng, and Y. Yin, "Coupling pulse eddy current sensor for deeper defects NDT," *Sens. Actuators A, Phys.*, vol. 293, pp. 189–199, Jul. 2019, doi: 10.1016/j.sna.2019.03.029.

[72] R. Mardaninejad and M. S. Safizadeh, "Gas pipeline corrosion mapping through coating using pulsed eddy current technique," *Russian J. Nondestruct. Test.*, vol. 55, no. 11, pp. 858–867, Nov. 2019, doi: 10.1134/S1061830919110068.

[73] S. Denenberg, T. Dunford, Y. Sheiretov, S. Haque, B. Manning, A. Washabaugh, and N. Goldfine, "Advancements in imaging corrosion under insulation for piping and vessels," *Mater. Eval.*, vol. 73, no. 7, pp. 987–995, Jul. 2015.

[74] N. Yusa, T. Tomizawa, H. Song, and H. Hashizume, "Probability of detection analyses of eddy current data for the detection of corrosion," *Mater. Sci.*, vol. 4, pp. 3–7, 2018, doi: 10.26357/BNiD.2018.031.

[75] Y. Kuts, S. Maievskyi, A. Protasov, I. Lysenko, and O. Dugin, "Study of parametric transducer operation in pulsed eddy current non-destructive testing," in *Proc. IEEE 38th Int. Conf. Electron. Nanotechnol. (ELNANO)*, Apr. 2018, pp. 24–26.

[76] M. Ricci, G. Silipigni, L. Ferrigno, M. Laracca, I. D. Adewale, and G. Y. Tian, "Evaluation of the lift-off robustness of eddy current imaging techniques," *NDT E, Int.*, vol. 85, pp. 43–52, Jan. 2017, doi: 10.1016/j.ndteint.2016.10.001.

[77] Z. Jin, Y. Meng, R. Yu, R. Huang, M. Lu, H. Xu, X. Meng, Q. Zhao, Z. Zhang, A. Peyton, and W. Yin, "Methods of controlling lift-off in conductivity invariance phenomenon for eddy current testing," *IEEE Access*, vol. 8, pp. 122413–122421, 2020, doi: 10.1109/ACCESS.2020.3007216.

[78] X. Chen, J. Li, and Z. Wang, "Inversion method in pulsed eddy current testing for wall thickness of ferromagnetic pipes," *IEEE Trans. Instrum. Meas.*, vol. 69, no. 12, pp. 9766–9773, Dec. 2020, doi: 10.1109/TIM.2020.3005114.

[79] A. Sophian, G. Tian, and M. Fan, "Pulsed eddy current non-destructive testing and evaluation: A review," *Chin. J. Mech. Eng.*, vol. 30, no. 3, pp. 500–514, 2017, doi: 10.1007/s10033-017-0122-4.

[80] A. Sophian, F. Nafiah, T. S. Gunawan, N. A. M. Yusof, and A. Al-Kelabi, "Machine-learning-based evaluation of corrosion under insulation in ferromagnetic structures," *IIUM Eng. J.*, vol. 22, no. 2, pp. 226–233, Jul. 2021, doi: 10.31436/iiumej.v22i2.1692.

[81] L. Hewing, J. Kabzan, and M. N. Zeilinger, "Cautious model predictive control using Gaussian process regression," *IEEE Trans. Control Syst. Technol.*, vol. 28, no. 6, pp. 2736–2743, Nov. 2020, doi: 10.1109/TCST.2019.2949757.

[82] M. Sharifzadeh, A. Sikinioti-Lock, and N. Shah, "Machine-learning methods for integrated renewable power generation: A comparative study of artificial neural networks, support vector regression, and Gaussian process regression," *Renew. Sustain. Energy Rev.*, vol. 108, pp. 513–538, Jul. 2019, doi: 10.1016/j.rser.2019.03.040.

[83] E. Schulz, M. Speekenbrik, and A. Krause, "A tutorial on Gaussian process regression: Modelling, exploring, and exploiting functions," *J. Math. Psychol.*, vol. 85, pp. 1–16, Aug. 2018, doi: 10.1016/j.jmp.2018.03.001.

[84] V. L. Deringer, A. P. Bartók, N. Bernstein, D. M. Wilkins, M. Ceriotti, and G. Csányi, "Gaussian process regression for materials and molecules," *Chem. Rev.*, vol. 121, no. 16, pp. 10073–10141, Aug. 2021, doi: 10.1021/acs.chemrev.1c00022.

[85] J. Bailey, N. Long, and A. Hunze, "Eddy current testing with giant magnetoresistance (GMR) sensors and a pipe-encircling excitation for evaluation of corrosion under insulation," *Sensors*, vol. 17, no. 10, p. 2229, Sep. 2017, doi: 10.3390/s17102229.

[86] L. Jogschies *et al.*, "Recent developments of magnetoresistive sensors for industrial applications," *Sensors*, vol. 15, no. 11, pp. 28665–28689, Nov. 2015, doi: 10.3390/S151128665.

[87] D. Rifai, A. Abdalla, K. Ali, and R. Razali, "Giant magnetoresistance sensors: A review on structures and non-destructive eddy current testing applications," *Sensors*, vol. 16, no. 3, p. 298, Feb. 2016, doi: 10.3390/s16030298.

[88] M. Djamal and R. Ramli, "Giant magnetoresistance sensors based on ferrite material and its applications," in *Magnetic Sensors—Development Trends and Applications*. IntechOpen, Nov. 2017, pp. 111–132, doi: 10.5772/INTECHOPEN.70548.
[89] M.-D. Cubells-Beltrán, C. Reig, J. Madrenas, A. De Marcellis, J. Santos, S. Cardoso, and P. Freitas, "Integration of GMR sensors with different technologies," *Sensors*, vol. 16, no. 6, p. 939, Jun. 2016, doi: 10.3390/s16060939.
[90] R. Falque, "Automatic data interpretation and enhanced localization for inline remote field eddy current tools," Open Publications UTS Scholar, Tech. Rep., 2018.
[91] B. Łosiewicz, M. Popczyk, M. Szklarska, A. Smołka, P. Osak, and A. Budniok, "Application of the scanning Kelvin probe technique for characterization of corrosion interfaces," *Solid State Phenomena*, vol. 228, pp. 369–382, Mar. 2015, doi: 10.4028/www.scientific.net/SSP.228.369.
[92] R. Grothe, C. N. Liu, M. Baumert, O. Hesebeck, and G. Grundmeier, "Scanning Kelvin Probe Blister test measurements of adhesive delamination—Bridging the gap between experiment and theory," *Int. J. Adhes. Adhesives*, vol. 73, pp. 8–15, Mar. 2017, doi: 10.1016/J.IJADHADH.2016.11.006.
[93] M. Uebel, A. Vimalanandan, A. Laaboudi, S. Evers, M. Stratmann, D. Diesing, and M. Rohwerder, "Fabrication of robust reference tips and reference electrodes for Kelvin probe applications in changing atmospheres," *Langmuir*, vol. 33, no. 41, pp. 10807–10817, Oct. 2017, doi: 10.1021/acs.langmuir.7b02533.
[94] H. Zhang, "Radio frequency non-destructive testing and evaluation of defects under insulation," Tech. Rep., 2014.
[95] I. A. Shozib, A. Ahmad, A. M. Abdul-Rani, M. Beheshti, and A. A. Aliyu, "A review on the corrosion resistance of electroless Ni-P based composite coatings and electrochemical corrosion testing methods," *Corrosion Rev.*, vol. 40, no. 1, pp. 1–37, Feb. 2022, doi: 10.1515/corrrev-2020-0091.
[96] G. Ebrahimi, J. Neshati, and F. Rezaei, "An investigation on the effect of H_3PO_4 and HCl-doped polyaniline nanoparticles on corrosion protection of carbon steel by means of scanning Kelvin probe," *Prog. Organic Coatings*, vol. 105, pp. 1–8, Apr. 2017, doi: 10.1016/j.porgcoat.2016.12.016.
[97] C. Sun, S.-J. Ko, S. Jung, C. Wang, D. Lee, J.-G. Kim, and Y. Kim, "Visualization of electrochemical behavior in carbon steel assisted by machine learning," *Appl. Surf. Sci.*, vol. 563, Oct. 2021, Art. no. 150412, doi: 10.1016/j.apsusc.2021.150412.
[98] S. Brockhaus, M. Ginten, S. Klein, M. Teckert, O. Stawicki, D. Oevermann, S. Meyer, and D. Storey, "In-line inspection (ILI) methods for detecting corrosion in underground pipelines," *Underground Pipeline Corrosion, Detection, Anal. Prevention*, pp. 255–285, Jan. 2014, doi: 10.1533/9780857099266.2.255.
[99] S. Caines, F. Khan, J. Shirokoff, and W. Qiu, "Experimental design to study corrosion under insulation in harsh marine environments," *J. Loss Prevention Process Industries*, vol. 33, pp. 39–51, Jan. 2015, doi: 10.1016/j.jlp.2014.10.014.
[100] H. Taheri and A. A. Hassen, "Nondestructive ultrasonic inspection of composite materials: A comparative advantage of phased array ultrasonic," *Appl. Sci.*, vol. 9, no. 8, p. 1628, Apr. 2019, doi: 10.3390/app9081628.
[101] B. Yu, K. D. Tola, C. Lee, and S. Park, "Improving the ability of a laser ultrasonic wave-based detection of damage on the curved surface of a pipe using a deep learning technique," *Sensors*, vol. 21, no. 21, p. 7105, Oct. 2021, doi: 10.3390/s21217105.
[102] Y. He, B. Deng, H. Wang, L. Cheng, K. Zhou, S. Cai, and F. Ciampa, "Infrared machine vision and infrared thermography with deep learning: A review," *Infr. Phys. Technol.*, vol. 116, Aug. 2021, Art. no. 103754, doi: 10.1016/j.infrared.2021.103754.
[103] T. Kattenborn, J. Leitloff, F. Schiefer, and S. Hinz, "Review on convolutional neural networks (CNN) in vegetation remote sensing," *ISPRS J. Photogramm. Remote Sens.*, vol. 173, pp. 24–49, Mar. 2021, doi: 10.1016/j.isprsjprs.2020.12.010.
[104] A. Yassin, M. S. U. Rahman, and M. A. Abou-Khousa, "Imaging of near-surface defects using microwaves and ultrasonic phased array techniques," *J. Nondestruct. Eval.*, vol. 37, no. 4, pp. 1–8, Sep. 2018, doi: 10.1007/s10921-018-0526-9.
[105] J. Brizuela, J. Camacho, G. Cosarinsky, J. M. Iriarte, and J. F. Cruza, "Improving elevation resolution in phased-array inspections for NDT," *NDT E, Int.*, vol. 101, pp. 1–16, Jan. 2019, doi: 10.1016/j.ndteint.2018.09.002.
[106] M.-J. Jung, B.-C. Park, J.-H. Bae, and S.-C. Shin, "PAUT-based defect detection method for submarine pressure hulls," *Int. J. Nav. Archit. Ocean Eng.*, vol. 10, no. 2, pp. 153–169, Mar. 2018, doi: 10.1016/j.ijnaoe.2017.06.002.
[107] T. Latête, B. Gauthier, and P. Belanger, "Towards using convolutional neural network to locate, identify and size defects in phased array ultrasonic testing," *Ultrasonics*, vol. 115, Aug. 2021, Art. no. 106436, doi: 10.1016/j.ultras.2021.106436.
[108] A. Khan, A. Sohail, U. Zahoora, and A. S. Qureshi, "A survey of the recent architectures of deep convolutional neural networks," *Artif. Intell. Rev.*, vol. 53, no. 8, pp. 5455–5516, Apr. 2020, doi: 10.1007/s10462-020-09825-6.
[109] L. Alzubaidi, J. Zhang, A. J. Humaidi, A. Al-Dujaili, Y. Duan, O. Al-Shamma, J. Santamaría, M. A. Fadhel, M. Al-Amidie, and L. Farhan, "Review of deep learning: Concepts, CNN architectures, challenges, applications, future directions," *J. Big Data*, vol. 8, no. 1, pp. 1–74, Mar. 2021, doi: 10.1186/s40537-021-00444-8.
[110] A. Omar, "A note on NDT technology for detection of defects in oil and gas pipes," *Int. J. Thermal Environ. Eng.*, vol. 12, no. 2, pp. 117–118, 2016, doi: 10.5383/ijtee.12.02.006.
[111] M. T. Ghasr, M. J. Horst, M. Lechuga, R. Rapoza, C. J. Renoud, and R. Zoughi, "Accurate one-sided microwave thickness evaluation of lined-fiberglass composites," *IEEE Trans. Instrum. Meas.*, vol. 64, no. 10, pp. 2802–2812, Oct. 2015, doi: 10.1109/TIM.2015.2426352.
[112] G. N. Jawad and M. F. Akbar, "IFFT-based microwave non-destructive testing for delamination detection and thickness estimation," *IEEE Access*, vol. 9, pp. 98561–98572, 2021, doi: 10.1109/ACCESS.2021.3095105.
[113] T. D. Carrigan, B. E. Forrest, H. N. Andem, K. Gui, L. Johnson, J. E. Hibbert, B. Lennox, and R. Sloan, "Nondestructive testing of non-metallic pipelines using microwave reflectometry on an in-line inspection robot," *IEEE Trans. Instrum. Meas.*, vol. 68, no. 2, pp. 586–594, Feb. 2019, doi: 10.1109/TIM.2018.2847780.
[114] M. S. Ur Rahman, A. Yassin, and M. A. Abou-Khousa, "Microwave imaging of thick composite structures using circular aperture probe," *Meas. Sci. Technol.*, vol. 29, no. 9, Aug. 2018, Art. no. 095403, doi: 10.1088/1361-6501/aad2cf.
[115] S. Lenka, "Corrosion under insulation (CUI)-inspection technique and prevention," Indian National Seminar Exhibition on Non-Destructive Evaluation, Thiruvananthapuram, India, Tech. Rep., 2017, pp. 97–103.
[116] Z. Li, A. Haigh, C. Soutis, A. Gibson, and P. Wang, "A review of microwave testing of glass fibre-reinforced polymer composites," *Nondestruct. Test. Eval.*, vol. 34, no. 4, pp. 429–458, Oct. 2019, doi: 10.1080/10589759.2019.1605603.
[117] A. J. K. M. Firdaus, R. Sloan, C. I. Duff, M. Wielgat, and J. F. Knowles, "Microwave nondestructive evaluation of thermal barrier coated turbine blades using correlation analysis," in *Proc. 46th Eur. Microw. Conf. (EuMC)*, Oct. 2016, pp. 520–523, doi: 10.1109/EuMC.2016.7824394.
[118] Y.-H. Tsai, J. Wang, W.-T. Chien, C.-Y. Wei, X. Wang, and S.-H. Hsieh, "A BIM-based approach for predicting corrosion under insulation," *Autom. Construction*, vol. 107, Nov. 2019, Art. no. 102923, doi: 10.1016/j.autcon.2019.102923.
[119] S. Deif, L. Harron, and M. Daneshmand, "Out-of-sight salt-water concentration sensing using Chipless-RFID for pipeline coating integrity," in *IEEE MTT-S Int. Microw. Symp. Dig.*, Jun. 2018, pp. 367–370, doi: 10.1109/MWSYM.2018.8439237.
[120] S. Deif and M. Daneshmand, "Long array of microwave sensors for real-time coating defect detection," *IEEE Trans. Microw. Theory Techn.*, vol. 68, no. 7, pp. 2856–2866, Jul. 2020, doi: 10.1109/TMTT.2020.2973385.
[121] S. M. Bejjavarapu and F. Simonetti, "An experimental model for guided microwave backscattering from wet insulation in pipelines," *J. Nondestruct. Eval.*, vol. 33, no. 4, pp. 583–596, Oct. 2014, doi: 10.1007/s10921-014-0254-8.
[122] M. F. Akbar, R. Sloan, C. Duff, M. Wielgat, and J. Knowles, "Nondestructive testing of thermal barrier coated turbine blades using microwave techniques," *Mater. Eval.*, vol. 74, no. 4, pp. 543–551, 2016.
[123] B. Ahn, J. Kim, and B. Choi, "Artificial intelligence-based machine learning considering flow and temperature of the pipeline for leak early detection using acoustic emission," *Eng. Fract. Mech.*, vol. 210, pp. 381–392, Apr. 2019, doi: 10.1016/j.engfracmech.2018.03.010.
[124] T. S. Yee and M. F. Akbar, "Under insulation microwave non-destructive testing using dual-ridges open-ended rectangular waveguide," in *Proc. 11th Int. Conf. Robot., Vis., Signal Process. Power Appl.*, 2022, pp. 684–689, doi: 10.1007/978-981-16-8129-5_104.

[125] K. Abbasi and W. M. Alobaidi, "Estimation of time-of-flight based on threshold and peak analysis method for microwaves signals reflected from the crack," *Nondestruct. Test. Eval.*, vol. 33, no. 4, pp. 393–404, Oct. 2018, doi: 10.1080/10589759.2018.1495204.
[126] M. F. Isham, M. S. Leong, M. H. Lim, and Z. A. Ahmad, "Variational mode decomposition: Mode determination method for rotating machinery diagnosis," *J. Vibroengineering*, vol. 20, no. 7, pp. 2604–2621, Nov. 2018, doi: 10.21595/jve.2018.19479.
[127] Y. Diao, L. Yan, and K. Gao, "Improvement of the machine learning-based corrosion rate prediction model through the optimization of input features," *Mater. Des.*, vol. 198, Jan. 2021, Art. no. 109326, doi: 10.1016/j.matdes.2020.109326.
[128] R. Ramos, B. Valdez-Salas, R. Zlatev, M. S. Wiener, and J. M. B. Rull, "The discrete wavelet transform and its application for noise removal in localized corrosion measurements," *Int. J. Corrosion*, vol. 2017, pp. 1–7, 2017, doi: 10.1155/2017/7925404.
[129] T. S. Yee, M. F. Akbar, N. A. Ghazali, and M. F. P. Mohamed, "Defects detection using complementary split ring resonator with microstrip patch antenna," in *Proc. 11th Int. Conf. Robot., Vis., Signal Process. Power Appl.*, 2022, pp. 625–631, doi: 10.1007/978-981-16-8129-5_95.
[130] K. Sudheera and N. M. Nandhitha, "Application of Hilbert transform for flaw characterization in ultrasonic signals," *Indian J. Sci. Technol.*, vol. 8, no. 13, pp. 1–6, Jul. 2015, doi: 10.17485/ijst/2015/v8i13/56303.
[131] Z. Li, Y. Jiang, Q. Guo, C. Hu, and Z. Peng, "Multi-dimensional variational mode decomposition for bearing-crack detection in wind turbines with large driving-speed variations," *Renew. Energy*, vol. 116, pp. 55–73, Feb. 2018, doi: 10.1016/j.renene.2016.12.013.
[132] M. Zhang, Z. Jiang, and K. Feng, "Research on variational mode decomposition in rolling bearings fault diagnosis of the multistage centrifugal pump," *Mech. Syst. Signal Process.*, vol. 93, pp. 460–493, Sep. 2017, doi: 10.1016/j.ymssp.2017.02.013.
[133] R. R. Zebari, A. M. Abdulazeez, D. Q. Zeebaree, D. A. Zebari, and J. N. Saeed, "A comprehensive review of dimensionality reduction techniques for feature selection and feature extraction," *J. Appl. Sci. Technol. Trends*, vol. 1, no. 2, pp. 56–70, May 2020, doi: 10.38094/jastt1224.
[134] T. Mehmood and B. Ahmed, "The diversity in the applications of partial least squares: An overview," *J. Chemometrics*, vol. 30, no. 1, pp. 4–17, Jan. 2016, doi: 10.1002/cem.2762.
[135] C. T. Ser, P. Žuvela, and M. W. Wong, "Prediction of corrosion inhibition efficiency of pyridines and quinolines on an iron surface using machine learning-powered quantitative structure-property relationships," *Appl. Surf. Sci.*, vol. 512, May 2020, Art. no. 145612, doi: 10.1016/j.apsusc.2020.145612.
[136] M. F. Akbar, G. N. Jawad, L. D. Rashid, and R. Sloan, "Nondestructive evaluation of coatings delamination using microwave time domain reflectometry technique," *IEEE Access*, vol. 8, pp. 114833–114841, 2020, doi: 10.1109/ACCESS.2020.3003829.
[137] N.-D. Hoang, "Image processing-based pitting corrosion detection using Metaheuristic optimized multilevel image thresholding and machine-learning approaches," *Math. Problems Eng.*, vol. 2020, pp. 1–19, May 2020, doi: 10.1155/2020/6765274.
[138] A. Ali, A. Albasir, and O. M. Ramahi, "Microwave sensor for imaging corrosion under coatings utilizing pattern recognition," in *Proc. IEEE Int. Symp. Antennas Propag. (APSURSI)*, Jun. 2016, pp. 951–952, doi: 10.1109/APS.2016.7696184.
[139] N. B. Erichson, A. Mendible, S. Wihlborn, and J. N. Kutz, "Randomized nonnegative matrix factorization," *Pattern Recognit. Lett.*, vol. 104, pp. 1–7, Mar. 2018, doi: 10.1016/j.patrec.2018.01.007.
[140] R. Kannan, G. Ballard, and H. Park, "A high-performance parallel algorithm for nonnegative matrix factorization," *ACM SIGPLAN Notices*, vol. 51, no. 8, pp. 1–11, Nov. 2016, doi: 10.1145/3016078.2851152.
[141] Z. Li, J. Tang, and X. He, "Robust structured nonnegative matrix factorization for image representation," *IEEE Trans. Neural Netw. Learn. Syst.*, vol. 29, no. 5, pp. 1947–1960, May 2018, doi: 10.1109/TNNLS.2017.2691725.
[142] D. P. Varikuti, S. Genon, A. Sotiras, H. Schwender, F. Hoffstaedter, K. R. Patil, C. Jockwitz, S. Caspers, S. Moebus, K. Amunts, C. Davatzikos, and S. B. Eickhoff, "Evaluation of non-negative matrix factorization of grey matter in age prediction," *NeuroImage*, vol. 173, pp. 394–410, Jun. 2018, doi: 10.1016/j.neuroimage.2018.03.007.
[143] S. Mei, H. Yang, and Z. Yin, "An unsupervised-learning-based approach for automated defect inspection on textured surfaces," *IEEE Trans. Instrum. Meas.*, vol. 67, no. 8, pp. 1266–1277, Jun. 2018, doi: 10.1109/TIM.2018.2795178.
[144] B. Qin, C. Hu, and S. Huang, "Target/background classification regularized nonnegative matrix factorization for fluorescence unmixing," *IEEE Trans. Instrum. Meas.*, vol. 65, no. 4, pp. 874–889, Apr. 2016, doi: 10.1109/TIM.2016.2516318.
[145] F. Y. Osisanwo, J. E. T. Akinsola, O. Awodele, J. O. Hinmikaiye, O. Olakanmi, and J. Akinjobi, "Supervised machine learning algorithms: Classification and comparison," *Int. J. Comput. Trends Technol.*, vol. 48, no. 3, pp. 128–138, Jun. 2017, doi: 10.14445/22312803/IJCTT-V48P126.
[146] M. M. Mehmet?sahin and R. Erol, "A comparative study of neural networks and ANFIS for forecasting attendance rate of soccer games," *Math. Comput. Appl.*, vol. 22, no. 4, p. 43, Nov. 2017, doi: 10.3390/mca22040043.
[147] X. Yuan, B. Huang, Y. Wang, C. Yang, and W. Gui, "Deep learning-based feature representation and its application for soft sensor modeling with variable-wise weighted SAE," *IEEE Trans. Ind. Informat.*, vol. 14, no. 7, pp. 3235–3243, Jul. 2018, doi: 10.1109/TII.2018.2809730.
[148] J.-S. Chou, N.-T. Ngo, and W. K. Chong, "The use of artificial intelligence combiners for modeling steel pitting risk and corrosion rate," *Eng. Appl. Artif. Intell.*, vol. 65, pp. 471–483, Oct. 2017, doi: 10.1016/j.engappai.2016.09.008.
[149] A. Ali, B. Hu, and O. Ramahi, "Intelligent detection of cracks in metallic surfaces using a waveguide sensor loaded with metamaterial elements," *Sensors*, vol. 15, no. 5, pp. 11402–11416, May 2015, doi: 10.3390/s150511402.
[150] M. M. Khan, A. A. Mokhtar, and H. Hussin, "A neural based fuzzy logic model to determine corrosion rate for carbon steel subject to corrosion under insulation," *Appl. Mech. Mater.*, vols. 789–790, pp. 526–530, Sep. 2015, doi: 10.4028/www.scientific.net/AMM.789-790.526.
[151] N. Morizet, N. Godin, J. Tang, E. Maillet, M. Fregonese, and B. Normand, "Classification of acoustic emission signals using wavelets and random forests : Application to localized corrosion," *Mech. Syst. Signal Process.*, vols. 70–71, pp. 1026–1037, Mar. 2016, doi: 10.1016/j.ymssp.2015.09.025.
[152] Y. Pan, X. Zhang, M. Sun, and Q. Zhao, "Object-based and supervised detection of potholes and cracks from the pavement images acquired by UAV," *Int. Arch. Photogramm., Remote Sens. Spatial Inf. Sci.*, vol42, pp. 209–217, Sep. 2017, doi: 10.5194/isprs-archives-XLII-4-W4-209-2017.
[153] K.-W. Liao and Y.-T. Lee, "Detection of rust defects on steel bridge coatings via digital image recognition," *Autom. Construct.*, vol. 71, pp. 294–306, Nov. 2016, doi: 10.1016/j.autcon.2016.08.008.
[154] A. N. Hoshyar, M. Rashidi, R. Liyanapathirana, and B. Samali, "Algorithm development for the non-destructive testing of structural damage," *Appl. Sci.*, vol. 9, no. 14, p. 2810, Jul. 2019, doi: 10.3390/app9142810.
[155] M. Agarwal, K. K. Rao, K. Vaidya, and S. Bhattacharya, "ML-MOC: Machine learning (kNN and GMM) based membership determination for open clusters," *Monthly Notices Roy. Astronomical Soc.*, vol. 502, no. 2, pp. 2582–2599, Feb. 2021, doi: 10.1093/mnras/stab118.
[156] J. Heil, V. Häring, B. Marschner, and B. Stumpe, "Advantages of fuzzy k-means over k-means clustering in the classification of diffuse reflectance soil spectra: A case study with west African soils," *Geoderma*, vol. 337, pp. 11–21, Mar. 2019, doi: 10.1016/j.geoderma.2018.09.004.
[157] K. H. Memon and D.-H. Lee, "Generalised kernel weighted fuzzy c-means clustering algorithm with local information," *Fuzzy Sets Syst.*, vol. 340, pp. 91–108, Jun. 2018, doi: 10.1016/j.fss.2018.01.019.
[158] Y. Ding and X. Fu, "Kernel-based fuzzy c-means clustering algorithm based on genetic algorithm," *Neurocomputing*, vol. 188, pp. 233–238, May 2016, doi: 10.1016/j.neucom.2015.01.106.

TAN SHIN YEE received the bachelor's degree in electronic engineering from Universiti Sains Malaysia (USM), Nibong Tebal, Malaysia, in 2020. She is currently pursuing the Ph.D. degree in microwave non-destructive testing with the School of Electrical and Electronic Engineering.

NAWAF H. M. M. SHRIFAN received the bachelor's degree in computer science and engineering from the University of Aden, Aden, Yemen, in 2006, and the MSc. and Ph.D. degrees from Universiti Sains Malaysia (USM), in 2017 and 2022, respectively. He is currently an Assistant Professor with the Department of Oil and Gas Engineering, Faculty of Oil and Minerals, University of Aden. His current research interests include microwave nondestructive testing, and computational intelligence algorithms.

AHMED JAMAL ABDULLAH AL-GBURI received the M.Eng. and Ph.D. degrees in electronics and computer engineering (telecommunication systems) from Universiti Teknikal Malaysia Melaka (UTeM), Malaysia, in 2017, and 2021, respectively. He is currently a Postdoctoral Fellow with the Microwave research Group (MRG), Faculty of d Electronics and Computer Engineering, UTeM. He has authored and coauthored a number of journals and proceedings. His research interests include electromagnetic bandgap (EBG), artificial magnetic conductor (AMC), frequency selective surface (FSS), UWB antennas, array antennas, and small antennas for UWB and 5G applications. He has received the Best Paper Award from the IEEE Community and won a number of Gold, Silver, and Bronze medals in international and local competitions.

NOR ASHIDI MAT ISA received the B.Eng. degree (Hons.) in electrical and electronic engineering and the Ph.D. degree in electronic engineering (majoring in image processing and artificial neural network) from Universiti Sains Malaysia (USM), in 1999 and 2003, respectively. He is currently a Professor with the School of Electrical and Electronic Engineering, USM. He has published more than 180, 217 and 294 articles indexed in WoS-ISI (H-index 30), Scopus (H-index 36), and Google Scholar (H-Index 42), respectively. His research interests include intelligent systems, image processing, neural networks, computational intelligence, and medical image processing. Due to his outstanding achievement in research, he gained recognition, both national and internationally. He was recognized as a top 2% researcher in category—Citation Impact in Single Calendar Years 2019 and 2020 by Stanford University, USA, in 2019 and 2020, and Top Research Scientist Malaysia (TRSM) by Akademi Sains Malaysia (ASM), in 2020.

MUHAMMAD FIRDAUS AKBAR (Member, IEEE) received the B.Sc. degree in communication engineering from International Islamic University Malaysia (IIUM), Malaysia, in 2010, and the M.Sc. and Ph.D. degrees from The University of Manchester, Manchester, U.K, in 2012 and 2018, respectively. From 2010 to 2011, he was with Motorola Solutions, Pulau Pinang, Malaysia, as a Research and Development Engineer. From 2012 to 2014, he was an Electrical Engineer with Usains Infotech Sdn Bhd, Penang. He is currently a Senior Lecturer with Universiti Sains Malaysia (USM). He is also the Founder and the Director of USM start-up company, Visionlytics Sdn Bhd. His current research interests include electromagnetics, microwave nondestructive testing, microwave sensor, and imaging.